NUCLEAR FUSION REACTIONS UNDER NON - MAXWELLIAN CONDITIONS

by

SANGEETA AGRAWAL

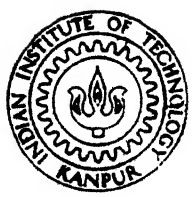

NUCLEAR ENGINEERING AND TECHNOLOGY PROGRAMME
INDIAN INSTITUTE OF TECHNOLOGY KANPUR
MARCH, 1986

NUCLEAR FUSION REACTIONS UNDER NON - MAXWELLIAN CONDITIONS

A Thesis Submitted
in Partial Fulfilment of the Requirements
for the Degree of

MASTER OF TECHNOLOGY

by

SANGEETA AGRAWAL

to the

NUCLEAR ENGINEERING AND TECHNOLOGY PROGRAMME
INDIAN INSTITUTE OF TECHNOLOGY KANPUR
MARCH, 1986

NETP-1986-M-AGA-NUC

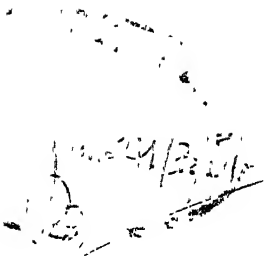

CERTIFICATE

This is to certify that the thesis entitled "NUCLEAR FUSION REACTIONS UNDER NON-MAXWELLIAN CONDITIONS" by SANGEETA AGRAWAL is a record of work carried out under my supervision and has not been submitted elsewhere for a degree.

M. S. Kalra

M. S. Kalra
Assistant Professor,
Nuclear Engg. and Tech. Programme,
Indian Institute of Technology,
Kanpur - 208016

March, 1986.

DEDICATED

TO

MY BELOVED PARENTS

ACKNOWLEDGEMENTS

I wish to express my thanks and deep sense of gratitude to my teacher, Dr. M.S. Kalra, who, with his patience and understanding, guided me at every stage of my thesis work. But for his help and encouragement, this work of mine would have been only a dream.

I would also like to thank all the other faculty members and staff of my department, who have all helped me, in one way or the other, during my stay in IITK.

For making my stay in IITK, a memorable one, thanks are also due to all my friends, especially Nivi, Rita, Tirumalai, Balaji and Ravi.

And finally, I would also like to acknowledge the contributions of Shri J.P. Gupta for typing this thesis.

SANGEETA AGRAWAL

ABSTRACT

Fusion reaction rates for DT, DD and DHe^3 reactions have been calculated for non-Maxwellian distribution of velocities. In particular, $\langle \sigma v \rangle$ values at various kinetic temperatures have been calculated for a two - temperature pseudo - Maxwellian distribution, which may approximately represent the velocities in a magnetic mirror reactor.

It is found that for the same kinetic temperature, a two - temperature distribution gives enhanced reaction rates between 5 to 15 keV for DT reaction and between 20 to 40 keV for DD and DHe^3 reactions. These are the temperature ranges of maximum practical interest. Calculations at other temperatures are also reported. It is found that at very high temperatures, the two - temperature distribution gives reduced reaction rates in contrast to the favourable behaviour at lower temperatures.

CONTENTS

NOMENCLATURE

v	Relative speed of the two species
$\vec{v}$	Relative velocity of the two species
$\vec{V}$	Velocity of the centre of mass
n_A	Number density of species A per unit volume
n_B	Number density of species B per unit volume
m_A	Mass of the species A
m_B	Mass of the species B
M	Total mass
μ	Reduced mass
$\sigma(v)$	Microscopic cross section for the binary reaction
T	Thermodynamic Temperature in energy
T_r	Radial temperature
T_z	Axial temperature
β	Temperature ratio parameter
$f_A\ (v_1)$	Normalized Maxwellian distribution function of speed for species A
$f_B\ (v_2)$	Normalized Maxwellian distribution function of speed for species B

$f_A(\vec{v}_1)$ Normalized Maxwellian distribution function of velocity for species A

$f_B(\vec{v}_2)$ Normalized Maxwellian distribution function of velocity for species B

LIST OF FIGURES

LIST OF TABLES

Chapter 1

INTRODUCTION

As is well known, in both the lightest and the heaviest nuclei, the mean binding energy per nucleon is less than that in the intermediate ones. Consequently, nuclear energy is released in the fission of heavy elements and in the fusion reactions of the lightest ones. The fusion reactions of practical interest at present in the nuclear fusion program are the following :

$$D + T \longrightarrow He^4\ (3.5\ MeV) + n\ (14.1\ MeV) \qquad (1.1)$$

$$D + D \longrightarrow T\ (1\ MeV) + p\ (3\ MeV) \qquad (1.2a)$$

$$D + D \longrightarrow He^3\ (0.8\ MeV) + n\ (2.5\ MeV) \qquad (1.2b)$$

$$D + He^3 \longrightarrow He^4\ (3.7\ MeV) + p\ (14.6\ MeV) \qquad (1.3)$$

For the above reactions to occur, the two reactant particles must overcome the Coulomb barrier. In thermonuclear fusion this is achieved by raising the temperature of the reacting species. For useful reaction rates, the temperatures required are 5 to 10 keV for the DT reaction, and 20 to 40 keV for the DD and DHe^3 reactions [1]. These are extremely high temperatures, of the order of 10^8 K, and

most of the difficulties of achieving nuclear fusion are related to this. In contrast, we note that a fission reaction between a neutron and, say, a uranium nucleus, can proceed at room temperature, because neutron is not a charged particle.

The reacting mixtures in Eqs. 1.1 to 1.3 become fully ionized plasma at temperatures of the order of 10^8 K. Using the cross sections for the reactions under consideration, the reaction rates can be calculated if the velocity distributions of the reacting species are known. The reaction rates are generally calculated by assuming Maxwellian distribution of velocities of the two reacting species [1].

Our purpose in this work is to calculate the reaction rates of the reactions listed in Eqs. 1.1 to 1.3 if the velocity distributions deviate from the Maxwellian. This can be considered of some practical interest in view of the fact that velocity distributions in fusion reactors may be generally considered as different from Maxwellian, even though close to it.

For this purpose, we analyze in detail the methods of reaction rate calculations in Chapter 2, and develop appropriate equations for calculating the reaction rates under non-Maxwellian velocity distributions. Detailed calculations are carried out for a two - temperature pseudo - Maxwellian distribution. The results are reported and discussed in Chapter 3.

Chapter 2

ANALYSIS FOR REACTION RATE CALCULATIONS

2.1 THE BASIC EQUATIONS FOR BINARY REACTION RATES

We consider a system containing any number of species of particles, and direct our attention on two particular species A and B, and infact on a particular binary reaction between these two species. Let n_A and n_B be the number densities per unit volume of the two species, respectively, at a particular point under consideration, and $f_A(\vec{v_1})$ and $f_B(\vec{v_2})$ be their normalized velocity distribution functions at the same point, i.e.,

$$\int f_A(\vec{v_1})\, d^3v_1 = \int f_B(\vec{v_2})\, d^3v_2 = 1 \qquad (2.1)$$

Here d^3v_1 and d^3v_2 are infinitesimal volume elements in the velocity spaces. For example, in cartesian coordinates, $d^3v_1 = dv_{x1} \cdot dv_{y1} \cdot dv_{z1}$. Choosing $\vec{v_1}$ for the velocity space of species A, and $\vec{v_2}$ for that of species B is for the convenience of subsequent discussion, in which one wants to distinguish between the velocities of two particles even if the species A and B are taken to be the same.

Let $\sigma(v)$ be the microscopic cross section for the binary reaction under consideration, where

$$v = \left| \vec{v}_2 - \vec{v}_1 \right| \quad , \tag{2.2}$$

If one considers, as a target, a single particle of species A moving with velocity $\vec{v}_1$, and $n_B f_B (\vec{v}_2)\, d^3v_2 \left| \vec{v}_2 - \vec{v}_1 \right| = n_B f_B (\vec{v}_2)\, d^3v_2 . v$ as an incident beam of species B, the resulting removal rate from the beam will be

$$n_B f_B (\vec{v}_2)\, d^3v_2\, v\, \sigma(v) \quad . \tag{2.3}$$

Multiplying Eq. 2.3 by $n_A f_A (\vec{v}_1)\, d^3v_1$, the number of particles of species A per unit volume with velocities between $\vec{v}_1$ and $\vec{v}_1 + d\vec{v}_1$, and integrating over the respective velocity spaces, we obtain

$$R = n_A n_B \iint d^3v_1\, d^3v_2\, v\, \sigma(v)\, f_A(\vec{v}_1)\, f_B(\vec{v}_2) \tag{2.4}$$

where R is the number of interactions per unit volume per unit time of the desired type, and v is as in Eq. 2.2

An alternative way of obtaining (or looking at) Eq. 2.4 is to consider $n_A f_A (\vec{v}_1)\, d^3v_1 . v$ as the relative path length travelled by particles of species A (between $\vec{v}_1$ and $\vec{v}_1 + d\vec{v}_1$) in a unit spatial volume per unit time, and to consider $\sigma(v)\, n_B f_B (\vec{v}_2)\, d^3v_2$ as the macroscopic cross section due to particles of species B between $\vec{v}_2$ and $\vec{v}_2 + d\vec{v}_2$. Since the

latter gives the probability of interaction per unit (relative) path length travelled, multiplying the two and integrating over the velocity spaces yields Eq. 2.4.

Equation 2.4 for the volumetric reaction rate can be written as

$$R = n_A\, n_B\, \langle \sigma v \rangle \quad , \tag{2.4a}$$

where

$$\langle \sigma v \rangle = \iint d^3v_1\, d^3v_2\, v\, \sigma(v)\, f_A(\vec{v}_1)\, f_B(\vec{v}_2) \tag{2.4b}$$

If A and B refer to the same species, $f_A(\vec{v}_1)$ and $f_B(\vec{v}_2)$ will be replaced by the same distributions, $f(\vec{v}_1)$ and $f(\vec{v}_2)$, and Eq. 2.4a will read

$$R = \frac{1}{2}\, n^2\, \langle \sigma v \rangle \quad , \tag{2.4c}$$

where n is the total number of particles per unit volume of the single species under consideration. The appearance of the factor 1/2 in Eq. 2.4c is easily explained on the basis of every interaction having been counted twice when considering a single species of total number density n [1,6]. Alternatively, one can first take $n_A = n_B = n/2$, and consider the interaction between these two halves leading to $R_1 = (1/4)\, n^2\, \langle \sigma v \rangle$. One can then add to it successive contributions from within each half and so on, finally leading to Eq. 2.4c.

2.2 ASSUMPTIONS AND THEIR VALIDITY FOR FUSION REACTIONS

In deriving Eq. 2.4 for the volumetric reaction rate, R, various assumptions have been implicitly made. Some of the (more obvious) assumptions, and their validity for fusion reaction rate calculations, are briefly discussed below.

(1) Eq. 2.4 assumes that the particles of species A and B can be considered as classical particles, i.e. as localized wave packets whose extensions are small compared to the average interparticle distance. This will be realized if the average de Broglie wavelength, λ_d, is much less than the average interparticle distance, $n^{-1/3}$ [12] :

$$\lambda_d \, n^{1/3} << 1 \quad , \tag{2.5}$$

$$\lambda_d = \frac{h}{mv} \quad , \tag{2.5a}$$

where n is the particle density, h Planck's constant, m the mass of the particles (ions in a fusion reaction), and v is an average speed, say, the rms speed of the particles. If the condition 2.5 is not satisfied, the linear dependence of R on n_A and n_B (separately) in Eq. 2.4 will breakdown, even if suitable definitions of other variables can be arrived at. For a fusion reaction at say 10 keV, it is easily seen that $\lambda_d \sim 10^{-13}$ m which is sufficiently less than the interparticle distance even at $n = 10^{31}$ m^{-3}, a typical particle density for

inertial fusion. (Some of the constants needed for these estimations are given in Appendix C).

(2) The range of the forces leading to the reaction under consideration in Eq. 2.4 should be sufficiently less than the interparticle distances. The best way to check it is :

$$\sigma^{1/2}\, n^{1/3} \ll 1 \qquad (2.6)$$

For fusion reactions, the highest value of σ is 5×10^{-28} m^2, and the condition 2.6 is seen to be satisfied even in the worst case of inertial fusion. It may be mentioned that if condition 2.6 is not satisfied, again the linear dependence of R on n_A and n_B will breakdown, i.e. some other term(s) in the rhs of Eq. 2.4 will also have some dependence on n_A and n_B.

(3) For Eq. 2.4 to be valid, the velocity of a particle should not be correlated to its position with respect to another particle. For this to be realized, there should be no long-range interparticle forces. This obviously is not valid for plasmas. However, if the average potential energy, <PE>, in the system per unit volume is sufficiently less than the average kinetic energy, <KE>, per unit volume, the effect of correlations on the reaction rate can be ignored [6,4]. This is equivalent to the condition that the Debye length, λ_D, be large compared to the interparticle distance [2,3] :

$$\lambda_D \, n^{1/3} \gg 1, \tag{2.7}$$

where

$$\lambda_D = \left(\frac{\varepsilon_o T}{n e^2} \right)^{1/2}, \tag{2.7a}$$

ε_o = permittivity of free space,

T = temperature, in J, and

e = electronic charge.

It is seen that for inertial fusion ($n \backsim 10^{31}$ m^{-3}, $T \backsim 10$ keV), $\lambda_D \, n^{1/3} \backsim 1$. Hence the condition 2.7 is not satisfied, and correlation corrections may be required. However, all the calculations in this work relate to magnetic fusion, in particular, to velocity distributions appropriate to mirror systems. For magnetic fusion, the condition 2.7 can be easily seen to be satisfied.

(4) It should be mentioned that Eq. 2.4 gives only an expected reaction rates. For magnetic fusion smallest volume ΔV and time δt of interest are of the order of 10^{-9} m^3 and 10^{-3} s, respectively. For inertial fusion, the same may be $\backsim 10^{-18}$ m^3 and $\backsim 10^{-11}$ s. At T = 10 keV and densities of the order of 10^{21} m^{-3} and 10^{31} m^{-3} respectively, it can be seen that $R\Delta V\delta t \backsim 10^8$. Hence the expected rate will be close to the actual rate, fluctuations in $R\Delta V\delta t$ being of the order of $\sqrt{R\Delta V\delta t}$ [6].

(5) Relativistic corrections are completely negligible, average ion velocities in fusion plasmas being of the order of 10^6 m s^{-1}. The effect of external forces on fusion cross sections is ignored (However, see the next remark).

(6) Polarization effects are ignored, i.e., in the measurement or calculation of $\sigma(v)$, all allowable relative spin orientations of the interacting species are considered to be equally probable. (Oppositely polarized ions can enhance fusion cross sections by as much as a factor of two [11]. The external forces, for example, magnetic fields, do effect the state of polarization, generally acting as a depolarizing mechanism, and thus destroying the reaction enhancing effect of spin polarization.) If the state of polarization is clearly known, an appropriately weighted $\sigma(v)$ can be defined and Eq. 2.4 for reaction rate calculations can still be used.

2.3 $\langle \sigma v \rangle$ FOR MAXWELLIAN DISTRIBUTIONS

2.3.1 Three Dimensional Maxwellian Distribution

The three dimensional normalized Maxwellian distribution of velocities for, say, a species A, whose (peculiar) velocities are denoted by, say, $\vec{v_1}$, is given by:

$$f_A(\vec{v_1}) = \left(\frac{m_A}{2\pi T}\right)^{3/2} e^{-\frac{m_A v_1^2}{2T}}, \qquad (2.8)$$

from which it follows that the three dimensional Maxwellian distribution of speeds is

$$f_A(v_1) = 4\pi \left(\frac{m_A}{2\pi T}\right)^{3/2} e^{-\frac{m_A v_1^2}{2T}} v_1^2 \qquad (2.8a)$$

As usual, we use the same symbol for the velocity and speed distributions, even though the two functions are different. In Eqs. 2.8 and 2.8a, m_A is the mass of the particles (in Kg.) and T is the thermodynamic temperature (in J). Normalization is easily verified by integrating Eq. 2.8a w.r.t. v_1 from $v_1 = o$ to ∞ . Alternatively, in cartesian coordinates, v_1^2 in Eq. 2.8 can be replaced by $v_{x1}^2 + v_{y1}^2 + v_{z1}^2$ and integration performed w.r.t. v_{x1}, v_{y1} and v_{z1} from $-\infty$ to $+\infty$. In both cases, the result obtained is unity. It should also be pointed out that the distribution in Eq. 2.8a is for all solid angles. If it is written on the basis of per steradian, the factor 4π will not appear in the distribution function, but will reappear during integration over the entire solid angle.

In order to calculate $\langle\sigma v\rangle$ (see Eq. 2.4b) for two species A and B, both of which are at the same thermodynamic temperature T, the relative speed distribution between the two species can be written down using the basic laws of statistical mechanics [6], i.e. the same laws which yield Maxwellian distribution of individual species to begin with. This is obtained by replacing m in Eq. 2.8a by the reduced mass, μ :

$$\mu = \frac{m_A\, m_B}{m_A + m_B} \tag{2.9}$$

$$f_{AB}(v) = 4\pi \left(\frac{\mu}{2\pi T}\right)^{3/2} e^{-\frac{\mu v^2}{2T}} \cdot v^2 \tag{2.10}$$

where $v = \left|\vec{v}_2 - \vec{v}_1\right|$ is the relative speed as in Eq. 2.2. The meaning of $f_{AB}(v)$ is that $n_B f_{AB}(v)\, dv$ gives the number of particles of species B per unit volume whose relative speeds w.r.t. any given particle of species A are between v and v + dv. Alternatively, $n_A f_{AB}(v)\, dv$ can be interpreted reciprocally in a similar way. With this interpretation, it is then straightforward to rewrite Eq. 2.4b for this particular case of two species being at the same thermodynamic temperature T [1] :

$$\langle \sigma v \rangle_{3D} = 4\pi \left(\frac{\mu}{2\pi T}\right)^{3/2} \int_0^\infty dv\, v^3\, o(v)\, e^{-\frac{\mu v^2}{2T}} . \tag{2.11}$$

where 3D denotes 3-dimensional Maxwellian distribution.

We may mention here that the argument leading to Eq. (2.11) may appear somewhat subtle. In Section 2.4, we will obtain expressions for $\langle \sigma v \rangle$ for more general (non-equilibrium) velocity distributions. Eq. 2.11 will then appear as a special case. We may also mention here that Eq. 2.11 is the standard equation for calculating $\langle \sigma v \rangle$ for thermonuclear reactions [1,5].

2.3.2 One and Two Dimensional Maxwellian Distributions

Although one and two dimensional Maxwellian distributions are extreme cases and perhaps not of practical interest, we have calculated $\langle\sigma v\rangle$ for these distributions particularly to see that these limiting results are approached smoothly in computer calculations, as well as in analytical formulations. It is interesting, however, to note that if these limiting distributions could be approached in practice, it can lead to significant reaction enhancing effect in cases of practical importance (see Chapter 3 for details).

As has been remarked above, these limiting cases will appear as special cases of the more general expression for $\langle\sigma v\rangle$ to be developed in the next section. Our purpose here is to indicate that the argument used in Section 2.3.1 for three dimensional Maxwellian distribution can also be immediately extended to obtain $\langle\sigma v\rangle$ for one or two dimensional cases. For convenience, we denote the temperature T by T_z for 1-dimensional case, and by T_r for 2-dimensional case. By denoting the speeds by v_{1z} and v_{1r}, respectively for the 1-D and 2-D cases, we have the following speed distributions for species A :

$$f_A(v_{1z}) = 2\left(\frac{m_A}{2\pi T_z}\right)^{1/2} e^{-\frac{m_A v_{1z}^2}{2T_z}}, \qquad (2.12)$$

[1-dimensional Maxwellian distribution of speeds]

and

$$f_A(v_{1r}) = 2\pi \left(\frac{m_A}{2\pi T_r}\right) e^{-\frac{m_A v_{1r}^2}{2 T_r}} \cdot v_{1r} \qquad (2.13)$$

[2-dimensional Maxwellian distribution of speeds]

By using the same arguments as in Section 2.3.1, one can write respective f_{AB} (v) by replacing m_A in Eqs. 2.12 and 2.13 by the reduced mass, μ, and finally the following expressions for $\langle\sigma v\rangle$ can be obtained :

$$\langle\sigma v\rangle_{1D} = 2 \left(\frac{\mu}{2\pi T_z}\right)^{1/2} \int_0^\infty dv\, v\, \sigma(v)\, e^{-\frac{\mu v^2}{2T_z}} . \qquad (2.14)$$

and

$$\langle\sigma v\rangle_{2D} = \left(\frac{\mu}{T_r}\right) \int_0^\infty dv\, v^2\, \sigma(v)\, e^{-\frac{\mu v^2}{2T_r}} . \qquad (2.15)$$

2.4 TRANSFORMATION TO CM AND RELATIVE VELOCITY COORDINATES

In order to calculate $\langle\sigma v\rangle$ for two arbitrary velocity distributions $f_A(\vec{v}_1)$ and $f_B(\vec{v}_2)$, Eq. 2.4b has to be integrated over six variables - 3 for $\vec{v}_1$ and $\vec{v}_2$ each. As it stands, none of these integrations can be performed without making explicit use of $\sigma(v)$, because $v = |\vec{v}_2 - \vec{v}_1|$ contains all the six variables of integration. However, by changing the variables of integration from $\vec{v}_1$ and $\vec{v}_2$ to $\vec{V}$ and $\vec{v}$ (defined

below), five of the integrations can be performed as $\sigma(v)$ does not depend on them. Integration over v can then be performed analytically or computationally, making explicit use of $\sigma(v)$.

We define :

$$\vec{V} = \frac{m_A \vec{v}_1 + m_B \vec{v}_2}{m_A + m_B} \quad , \text{ and} \tag{2.16}$$

$$\vec{v} = \vec{v}_2 - \vec{v}_1 \quad . \tag{2.17}$$

It is immediately seen that $\vec{V}$ is the center of mass velocity, and $\vec{v}$ is the relative velocity, whose magnitude v we have used earlier. By changing the variables of integration to $\vec{V}$ and $\vec{v}$, Eq. 2.4b can be written as

$$\langle \sigma v \rangle = \iint d^3v \, d^3V \, v \, \sigma(v) \, f_A(\vec{V},\vec{v}) \, f_B(\vec{V}, \vec{v}) \left| \frac{\partial(\vec{v}_1, \vec{v}_2)}{\partial(\vec{V}, \vec{v})} \right| \tag{2.18}$$

where $\left| \frac{\partial(\vec{v}_1, \vec{v}_2)}{\partial(\vec{V}, \vec{v})} \right|$ is the magnitude of the Jacobian $\frac{\partial(\vec{v}_1, \vec{v}_2)}{\partial(\vec{V}, \vec{v})}$. It should be mentioned here that after the variables are changed, in writing Eq. 2.18, we have continued to denote the distribution functions by f_A and f_B, even though they are different functions. Further, the region of integration in 2.18 should corresponding to the region of integration in the original Eq. 2.4a.

The Jacobian mentioned above is evaluated in Appendix A, and its magnitude is seen to be unity. As a result,

$$\langle \sigma v \rangle = \iint d^3v\, d^3V\, f_A(\vec{v}, \vec{V})\, f_B(\vec{v}, \vec{V})\, v\, \sigma(v) \tag{2.19}$$

It is seen that in Eq. 2.19, integration w.r.t. d^3V can be performed in any convenient coordinates. However, for integration w.r.t. d^3v, one of the coordinates must be the magnitude of $\vec{v}$, i.e. v, so that two of three integrations involved can be obtained without using $\sigma(v)$. Spherical coordinates for d^3v will, therefore, generally be suitable.

2.5 A TWO-TEMPERATURE PSEUDO-MAXWELLIAN DISTRIBUTION

In the next section, we will develop an appropriate expression for $\langle \sigma v \rangle$ for a chosen non-Maxwellian distribution function of speeds. For this purpose, we choose a two-temperature pseudo-Maxwellian distribution function, which in some sense, can be used to characterize the velocity distributions in a mirror fusion reactor. This is based on having one temperature, T_z, characteristic of the velocity distributions along the magnetic field lines, and another temperature, T_r, characterizing the velocities perpendicular to the magnetic field lines. A normalized velocity distribution function of this kind for, say, a species A whose velocities are denoted by $\vec{v}_1$, can be written as follows :

$$f_A(\vec{v}_1) = \left(\frac{m_A}{2\pi T_z}\right)^{\frac{1}{2}} \left(\frac{m_A}{2\pi T_r}\right) e^{-\frac{m_A v_{1z}^2}{2T_z}} e^{-\frac{m_A v_{1r}^2}{2T_r}}, \qquad (2.20)$$

where v_{1z} = component of $\vec{v}_1$ parallel to the field lines, and

v_{1r} = component of $\vec{v}_1$ perpendicular to the field lines.

In Eq. 2.20 if we put,

$$T_z = T_r = T, \text{ and}$$

$$v_1^2 = v_{1r}^2 + v_{1z}^2 ,$$

We immediately get the 3-D Maxwellian distribution of Eq. 2.8. If we multiply Eq. 2.20 by $2\pi v_{1r} dv_{1r}$ and integrate from v_{1r} = o to ∞ , we get 1-D Maxwellian distribution of velocities :

$$f_A(\vec{v}_{1z}) = \left(\frac{m_A}{2\pi T_z}\right)^{\frac{1}{2}} e^{-\frac{m_A v_{1z}^2}{2 T_z}} \qquad (2.21)$$

It is to be noted that the velocity distribution of Eq. 2.21 above rightly differs from the corresponding speed distribution of Eq. 2.8 by a factor of 2. This is because the velocity $\vec{v}_{1z}$ will range from $-\infty$ to $+\infty$, while the speed v_{1z} will range from o to ∞ .

Similarly, if Eq. 2.20 is integrated over v_{1z} (from $-\infty$ to $+\infty$), 2-D Maxwellian distribution of velocities is obtained:

$$f_A(\vec{v}_{1r}) = \left(\frac{m_A}{2\pi T_r}\right) e^{-\frac{m_A v_{1r}^2}{2 T_r}} \qquad (2.22)$$

which again differs from the corresponding speed distribution of Eq. 2.13 by a factor of $2\pi v_{1r}$.

2.6 <σv> FOR THE PSEUDO-MAXWELLIAN DISTRIBUTION

In order to calculate <σv> for two species A and B, with velocity distribution as in Eq. 2.20, we first write a similar expression for $f_B(\vec{v}_2)$, taking T_z and T_r for species B to be the same as that for species A. (If this is not so, the method developed in Section 2.4, which is used below, will still be applicable. Only the details will be different and more involved.)

In general, in order to change to CM and relative velocity coordinates, Eqs. 2.16 and 2.17 will be solved for six components of $\vec{v}_1$ and $\vec{v}_2$ in terms of the six components of $\vec{V}$ and $\vec{v}$, and the resulting expressions will be utilized in $f_A(\vec{v}_1)$ and $f_B(\vec{v}_2)$ to obtain $f_A(\vec{v}, \vec{V})$ and $f_B(\vec{v}, \vec{V})$. Then, as pointed out earlier, five of the six integrations in the general expression for <σv> in Eq. 2.19 can be carried out without explicit use of σ(v).

The same procedure is, of course, applicable for the distribution being considered. However, the details are simplified for this particular case by noting that Eqs. 2.16 and 2.17 imply for z-component (see Appendix A) :

$$m_A v_{1z}^2 + m_B v_{2z}^2 = \mu v_z^2 + M V_z^2 \qquad (2.23)$$

where μ is the reduced mass as defined earlier and $M = m_A + m_B$. Relations similar to Eq. 2.23 will be valid for other components. As a result we also have,

$$m_A v_{1r}^2 + m_B v_{2r}^2 = \mu v_r^2 + M V_r^2 \qquad (2.23a)$$

Since only v_{1z}^2 and v_{1r}^2 occur in the pseudo-Maxmellian distribution of Eq. 2.20 under consideration here, it is easy to see, with the help of Eqs. 2.23 and 2.23a, that the Eq. 2.19 for $\langle\sigma v\rangle$ reduces to the following for the present case :

$$\langle\sigma v\rangle_{rz} = \frac{(m_A m_B)^{3/2}}{8\pi^3 T_z T_r^2} \iint d^3V d^3v \; v \; \sigma(v) \; e^{-\frac{MV_z^2}{2T_z}} e^{-\frac{MV_r^2}{2T_r}} e^{-\frac{\mu v_z^2}{2T_z}} e^{-\frac{\mu v_r^2}{2T_r}}, \qquad (2.24)$$

where we have put a subscript rz on $\langle\sigma v\rangle$ to indicate that this applies to the two-temperature distribution of Eq. 2.20.

As promised earlier, five of the six integrations involved in Eq. 2.24 can now be performed. This is done by writing d^3V in circular cylindrical coordinates (Fig. 1a) :

$$d^3V = V_r \, dV_r \, d\theta \, dV_z ,$$

and integrating with the following limits :

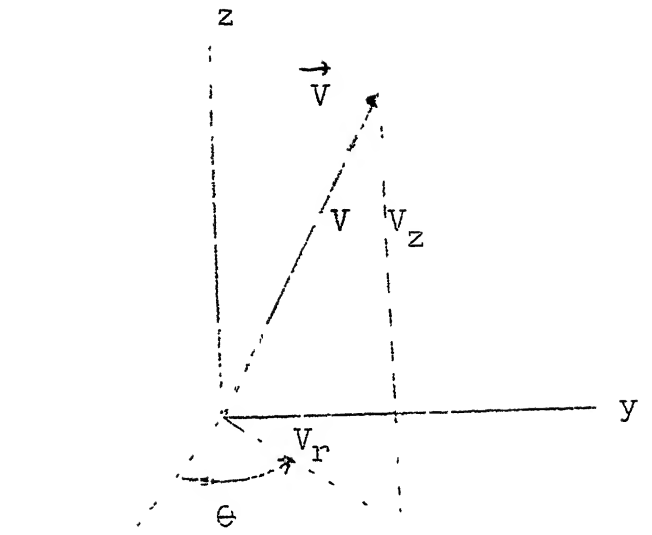

FIG.1a : Cylindrical coordinates for d^3v-integration in Eq.2.24

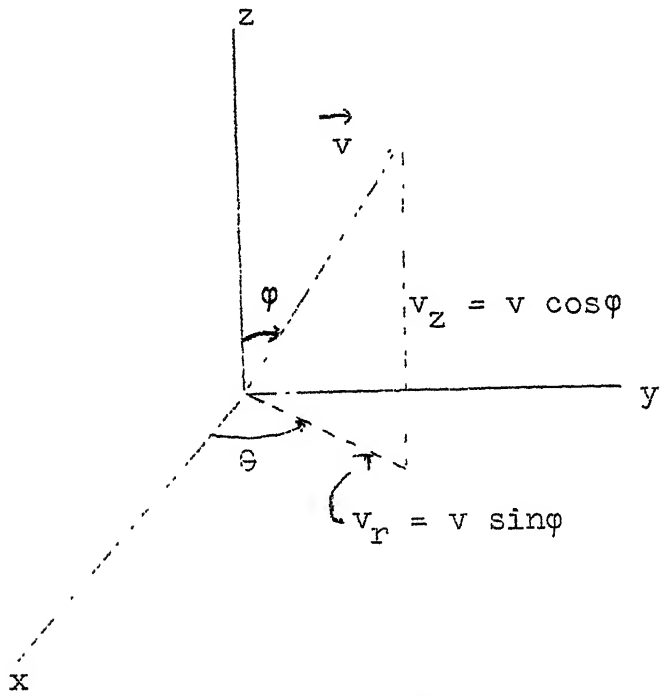

FIG.1b : Spherical coordinates for d^3v-integration in Eq. 2.24

V_r : o to ∞

V_z : $-\infty$ to ∞ , and

θ : o to 2π (see Fig. 1a)

Two of the integrations related to d^3v can be performed by writing d^3v in spherical coordinates (FIG. 1b) :

$$d^3v = v^2 \sin\varphi \, d\varphi \, d\theta \quad ,$$

and replacing v_z and v_r in Eq. 2.24 by :

$$v_z = v \cos\varphi \quad ,$$

$$v_r = v \sin\varphi \quad ,$$

with limits :

φ : o to π

θ : o to 2π (see FIG. 1b)

The resulting expression for $\langle\sigma v\rangle_{rz}$ is :

$$\langle\sigma v\rangle_{rz} = \sqrt{\frac{2}{\pi}} \frac{\mu^{3/2}}{T_z \, T_r^{1/2}} \int_0^{\infty} v^3 \, \sigma(v) \, e^{-\frac{\mu v^2}{2T_r}} \, I(v) \, dv \qquad (2.25)$$

where,

$$I(v) = \int_0^1 e^{\frac{\mu v^2 (T_z - T_r)}{2 \, T_z \, T_r}} \, . \, da \qquad (2.26)$$

[α here is related to the original integration w.r.t.φ by : $\alpha = \cos\varphi$; this integration can not be done analytically, but it does not require the knowledge of $\sigma(v)$].

If we use $T_r = T_z$ (= T) in Eq. 2.25, we immediately obtain $\langle\sigma v\rangle_{3D}$ as in Eq. 2.11. It is also possible to take limits in Eq. 2.25 as $T_r \longrightarrow o$, or as $T_z \longrightarrow o$, and obtain $\langle\sigma v\rangle_{1D}$ and $\langle\sigma v\rangle_{2D}$ of Eqs. 2.14 and 2.15 respectively. However, taking these limits is somewhat involved, and the desired results are more directly obtained by starting with Eqs. 2.21 and 2.22, instead of Eq. 2.20, and repeating the steps outlined in this section for these special cases.

2.7 BASIS OF COMPARISON FOR DIFFERENT $\langle\sigma v\rangle$'s

In order to compare $\langle\sigma v\rangle$'s for arbitrarily chosen velocity distributions $f_A(\vec{v_1})$ and $f_B(\vec{v_2})$, we define effective (kinetic) temperatures, T_A and T_B, of species A and B, respectively, as follows :

$$\frac{3}{2} T_A = \frac{1}{2} m_A \langle v_1^2 \rangle, \quad \text{and}$$

$$\frac{3}{2} T_B = \frac{1}{2} m_B \langle v_2^2 \rangle .$$

For the two-temperature pseudo-Maxwellian distributions [of the form given by Eq. 2.20], with the same T_r and T_z for the two species, these effective temperatures are easily seen to

be the same. Denoting this common effective (kinetic) temperature by T_K, we find by straightforward integration:

$$\frac{3}{2} T_K = T_r + \frac{1}{2} T_z \qquad (2.27)$$

Since T_K is a measure of the average kinetic energy per particle, it can be used as the basis for comparing $\langle \sigma v \rangle$ values for different distributions. Thus while varying T_r and T_z for the two-temperature distribution, we compare $\langle \sigma v \rangle$ values for a fixed T_K at a time.

2.8 TRANSFORMATION TO CONVENIENT (DIMENSIONLESS) PARAMETERS

To facilitate integration of Eqs. 2.25 and 2.26 in a more elegant form, and to facilitate some of the further discussions, we define

$$v_K \equiv \sqrt{\frac{3 T_K}{\mu}} \qquad (2.28)$$

where μ is the reduced mass. We then define the temperature ratio parameter, β, by :

$$\beta \equiv \frac{T_r}{T_z} \quad , \qquad (2.29)$$

and a dimensionless relative speed, ω. by :

$$\omega \equiv \frac{v}{v_K} \qquad (2.30)$$

These definitions, Eqs. 2.27 to 2.30, can be introduced into Eqs. 2.25 and 2.26. We first introduce Eqs. 2.27 and 2.29 to obtain :

$$\langle\sigma v\rangle_{rz} = \frac{1}{3}\sqrt{\frac{2}{3\pi}}\left(\frac{\mu}{T_K}\right)^{3/2}\int_0^\infty v^3\sigma(v)\, I(v,\beta)\, e^{\frac{-(2\beta+1)\mu\, v^2}{6\,\beta\, T_K}}\cdot dv\,, \tag{2.31}$$

where

$$I(v,\beta) = \int_0^1 e^{\frac{(1+2\beta)(1-\beta)\,\mu\, v^2}{6\,\beta\, T_K}\alpha^2}\cdot d\alpha \tag{2.32}$$

The above equations bring out the dependence of $\langle\sigma v\rangle_{rz}$ on T_K and β. If we now introduce Eqs. 2.28 and 2.30 in the last two equations, the later can be written as :

$$\langle\sigma v\rangle_{rz} = \sqrt{\frac{2}{\pi}}\cdot\frac{(2\beta+1)^{3/2}}{\beta}\cdot v_K\cdot\int_0^\infty \omega^3\,\sigma(\omega)\, I(\omega,\beta)\, e^{-\frac{\omega^2(2\beta+1)}{2\beta}}\cdot d\omega\,, \tag{2.33}$$

where

$$I(\omega,\beta) = \int_0^1 e^{\frac{(1+2\beta)(1-\beta)}{2\beta}\omega^2\,\alpha^2}\cdot d\alpha\,. \tag{2.34}$$

It is easily seen that the case $\beta = 1$ corresponds to $\langle\sigma v\rangle_{3D}$ of Eq. 2.11. It is also possible to show, with some involvement,

that the limits of Eq. 2.31 as $\beta \longrightarrow 0$ and $\beta \longrightarrow \infty$ exist and correspond, respectively, to $\langle\sigma v\rangle_{1D}$ and $\langle\sigma v\rangle_{2D}$ of Eqs. 2.14 and 2.15. To avoid repetition, appropriate expressions for these special cases are directly given in the next section, where we summarize the results of this chapter which are actually used in later calculations.

2.9 SUMMARY

For a two-temperature (pseudo-Maxwellian) distribution of velocities for species A,

$$f_A(\vec{v_1}) = \left(\frac{m_A}{2\pi T_z}\right)^{\frac{1}{2}} \cdot \left(\frac{m_A}{2\pi T_r}\right) \cdot e^{-\frac{m_A v_{1z}^2}{2 T_z}} \cdot e^{-\frac{m_A v_{1r}^2}{2 T_r}}, \tag{2.35}$$

and a similar distribution, $f_B(\vec{v_2})$, for species B with same T_z and T_r, we have

$$\langle\sigma v\rangle_{rz} = \sqrt{\frac{2}{\pi}} \cdot \frac{(2\beta+1)^{3/2}}{\beta} \cdot v_K \int_0^\infty \omega^3 \, \sigma(\omega) I(\omega,\beta) \cdot e^{-\frac{\omega^2(2\beta+1)}{2\beta}} \cdot d\omega, \tag{2.36}$$

where

$$I(\omega,\beta) = \int_0^1 e^{\frac{(1+2\beta)(1-\beta)}{2\beta}\omega^2 \alpha^2} \cdot d\alpha, \tag{2.37}$$

$$\beta = \frac{T_r}{T_z} \quad , \quad \frac{3}{2} T_K = T_r + \frac{1}{2} T_z \quad ,$$

$$v_K = \sqrt{\frac{3\ T_K}{\mu}} \quad ,$$

$$\omega = \frac{v}{v_K} \quad ,$$

$$v = \left| \vec{v_2} - \vec{v_1} \right| \quad , \quad \text{and}$$

$$\mu = \frac{m_A\ m_B}{m_A + m_B} \quad .$$

For $\beta = 1$,

$$\langle \sigma v \rangle_{3D} = 3 \sqrt{\frac{6}{\pi}}\ v_K \int_0^\infty \omega^3\ o(\omega)\ e^{-\frac{3}{2}\omega^2}\ d\omega \quad , \qquad (2.38)$$

for $\beta = o$

$$\langle \sigma v \rangle_{1D} = \sqrt{\frac{2}{\pi}}\ v_K \int_0^\infty \omega\ \sigma(\omega)\ e^{-\frac{\omega^2}{2}}\ d\omega \quad , \qquad (2.39)$$

and for $\beta = \infty$,

$$\langle \sigma v \rangle_{2D} = 2\ v_K \int_0^\infty \omega^2\ \sigma(\omega)\ e^{-\omega^2}\ d\omega \quad . \qquad (2.40)$$

Chapter 3

NUMERICAL COMPUTATIONS AND RESULTS

3.1 FUSION CROSS SECTIONS

3.1.1 Comparison of Experimental and Theoretical Data from Refs. [1], [7] and [8].

Tables 3.1 to 3.3 show experimentally measured values of σ_{DT}, σ_{DD} and σ_{DHe^3} at selected energy points. Here the incident particle is deuteron, and the target particle (triton, deuteron and He^3 respectively) is considered to be at rest in the laboratory system. The deuteron energy shown is, accordingly, the energy of the incident deuteron in the laboratory system. It is related to the relative velocity, v, of Section 2.9 by

$$\frac{1}{2} m_D v^2 = E_D \qquad (3.1)$$

where m_D is the deuteron mass.

It is seen that there is considerable difference in the cross sections from the two sources. For all calculations in this work we have used the cross sections from Ref. [1]. The values in Ref. [1] appear to have been arrived at by consulting different sources of experimental data, and were therefore considered to be better suited for our purpose. The detailed values are given in Appendix B. It should be noted that the

Table 3.1

Comparison of experimentally measured values of σ_{DT} from references [1] and [7]

S.No.	Deuteron energy E_D keV	$\sigma_{DT} \times 10^{28}$ from [1] m^2	$\sigma_{DT} \times 10^{28}$ from [7] m^2
1.	10	0.0018	0.0028
2.	50	1.40	1.5
3.	100	4.80	5.00
4.	500	1.05	0.630
5.	1000	0.310	0.345

Note : The values used for all calculations in this work are those of [1]. More detailed values are listed in Appendix B.

Table 3.2

Comparison of experimentally measured values of σ_{DD} from references [1] and [7]

S.No.	Deuteron energy E_D keV	$\sigma_{DD} \times 10^{30}$ from [1] m^2	$\sigma_{DD} \times 10^{30}$ from [7] m^2
1.	20	0.054	0.027
2.	60	1.3	0.75
3.	100	3.15	1.88
4.	200	6.4	4.0
5.	500	13.5	8.13
6.	1000	18.0	11.0

Note : The values used for all calculations in this work are those of [1]. More detailed values are listed in Appendix B.

Table 3.3

Comparison of experimentally measured values of σ_{DHe^3} from references [1] and [7]

S.No.	Deuteron energy, E_D keV	$\sigma_{DHe^3} \times 10^{30}$ from [1] m^2	$\sigma_{DHe^3} \times 10^{30}$ from [1] m^2
1.	40	0.0245	0.0291
2.	80	0.82	0.01
3.	100	1.97	1.843
4.	200	18.5	16.876
5.	600	64.8	60.0
6.	1000	24.4	25.521

Note : The values used for all calculations in this work are those of [1]. More detailed values are listed in Appendix B.

cross section σ_{DD} is the total cross section for both the reactions shown in Eqs. 1.2a and 1.2b.

On theoretical grounds, the cross section for a nuclear fusion reaction can be written as [1]:

$$\sigma(W) = \frac{A}{W} e^{-\sqrt{\frac{B}{W}}} \qquad (3.2)$$

where W = energy of the ineracting particles in center of mass system, and

A and B are constants.

Eq. 3.2 is particularly valid if W is well below the Coulomb barrier between the interacting particles. Theoretical expressions of A and B are available ([1], [8]). However, considering A and B as constants to be empirically determined, a least square fit between Eq. 3.2 and experimental data from Ref. [1] for DT reaction is shown in Fig. 3.1. For this purpose, only seven representative experimental values shown in Fig. 3.1 were used. The unweighted square error, ε_s, in the cross section values, given by,

$$\varepsilon_s = \Sigma (\sigma - \sigma_i)^2 \qquad (3.3)$$

was minimized, where σ is as calculated from Eq. 3.2 at the representative energy points, and σ_i is the corresponding experimental value. Here it should be mentioned that if A and

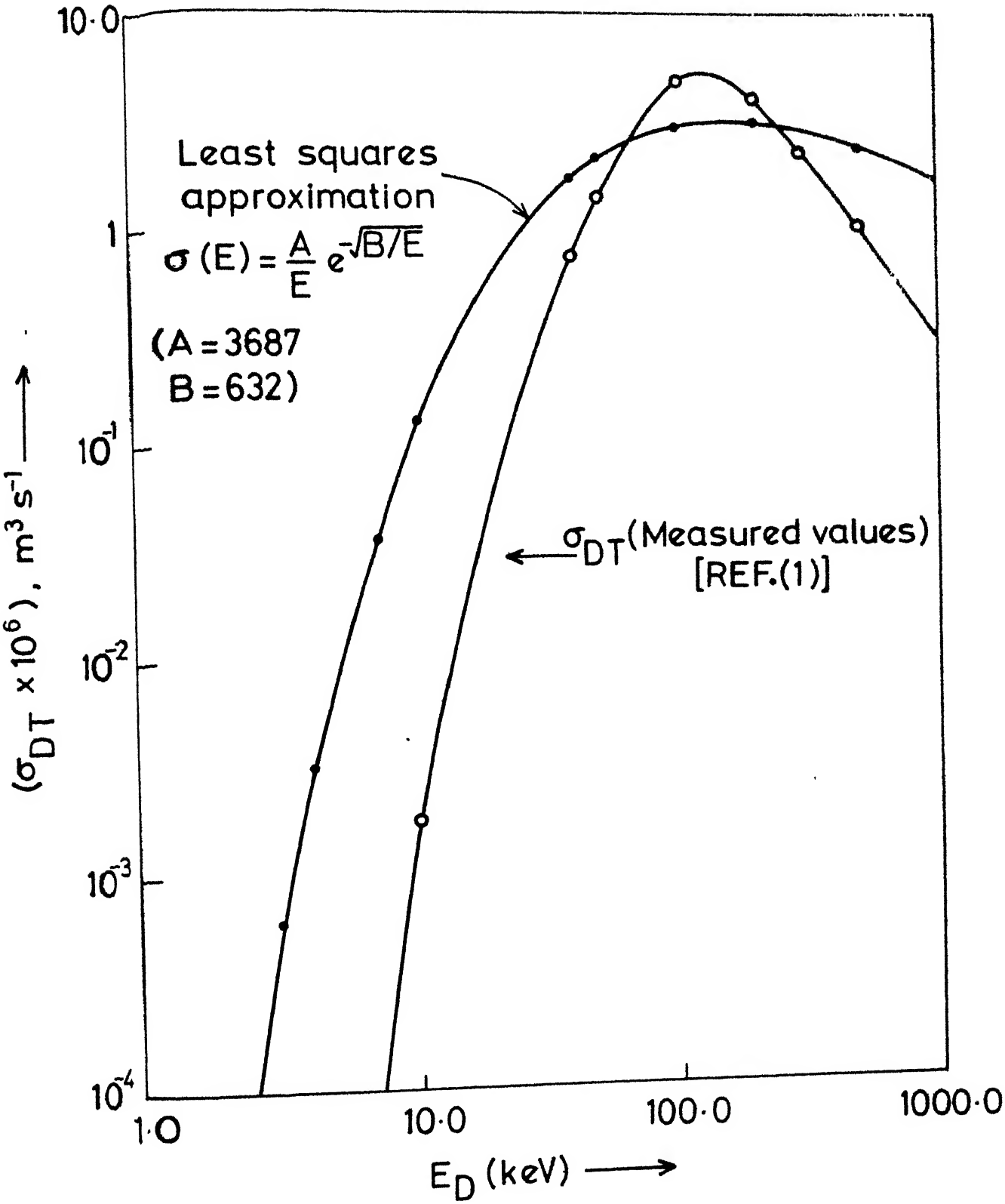

FIG. 3·1 Least squares approximation for σ_{DT}

B are considered as empirical constants, W in Eq. 3.2 can be replaced by deuteron energy, E_D, in the laboratory system.

It is seen in Fig. 3.1 that there is considerable difference between theoretical and experimental values, even if the constants A and B are determined empirically by least squares approximation. In this connection, we may also remark:

1. In Ref. [8], a theoretical expression for $\sigma(\omega)$ is given as follows :

$$\sigma(w) = a\, e^{-\sqrt{b/w}} \quad . \tag{3.4}$$

We considered this expression also, but the least squares error was more in comparison with that obtained from Eq. 3.2.

2. It appears that the values given in Ref. [1] actually correspond to a least square approximation between experimental data and a plot of $\ln (E_D\ \sigma(E_D))$ vs $E_D^{-1/2}$ according to Eq. 3.2. This plot is linear as can be seen from Eq. 3.2, by replacing W by E_D. We tried to check it. The values do not fall on a straightline. (There is some confusion here, probably due to a misprint, as in Ref. [1], it is stated that the plot $\ln (E_D\ \sigma(E_D))$ vs E_D is a straightline in accordance with Eq. 3.2; this is obviously not true.)

In any case, the cross section values given in Ref.[1] are most extensive, and are in reasonable agreement with limited experimental data consulted during this work. In Ref. [1], $\langle \sigma v \rangle$

values are also given for three dimensional Maxwellian distribution of velocities. Therefore, for the purposes of comparison with some of the calculations reported in this work, it was thought best to use the cross section data from Ref. [1], as summarized in Appendix B.

3.1.2 Interpolation between Experimental Values

For integrating Eq. 2.36, an energy interval of 1 keV was used. Since the values given in Appendix B are at intervals ranging from 1 to 100 keV, an interpolation had to be used. We considered both linear interpolation and an interpolation based on Eq. 3.2, with A and B determined using the two end values under consideration. The final results reported in this work are all based on this later interpolation scheme.

3.2 SOME REMARKS ON COMPUTER CALCULATIONS

An outline of the computer program used for calculating $\langle\sigma v\rangle_{rz}$ in accordance with Eqs. 2.36 to 2.40 is shown in Fig. 3.2. All integrations were done using Simpson's rule [13]:

$$\int_{x}^{x+h} f(x)\,dx = \frac{h}{2}\left[f(x+h) + f(x)\right] \qquad (3.4)$$

with an error term of the order of h^3. This was found to be adequate when used with an energy interval of 1 keV. However, for integrating Eq. 2.37, especially for low values of β, very

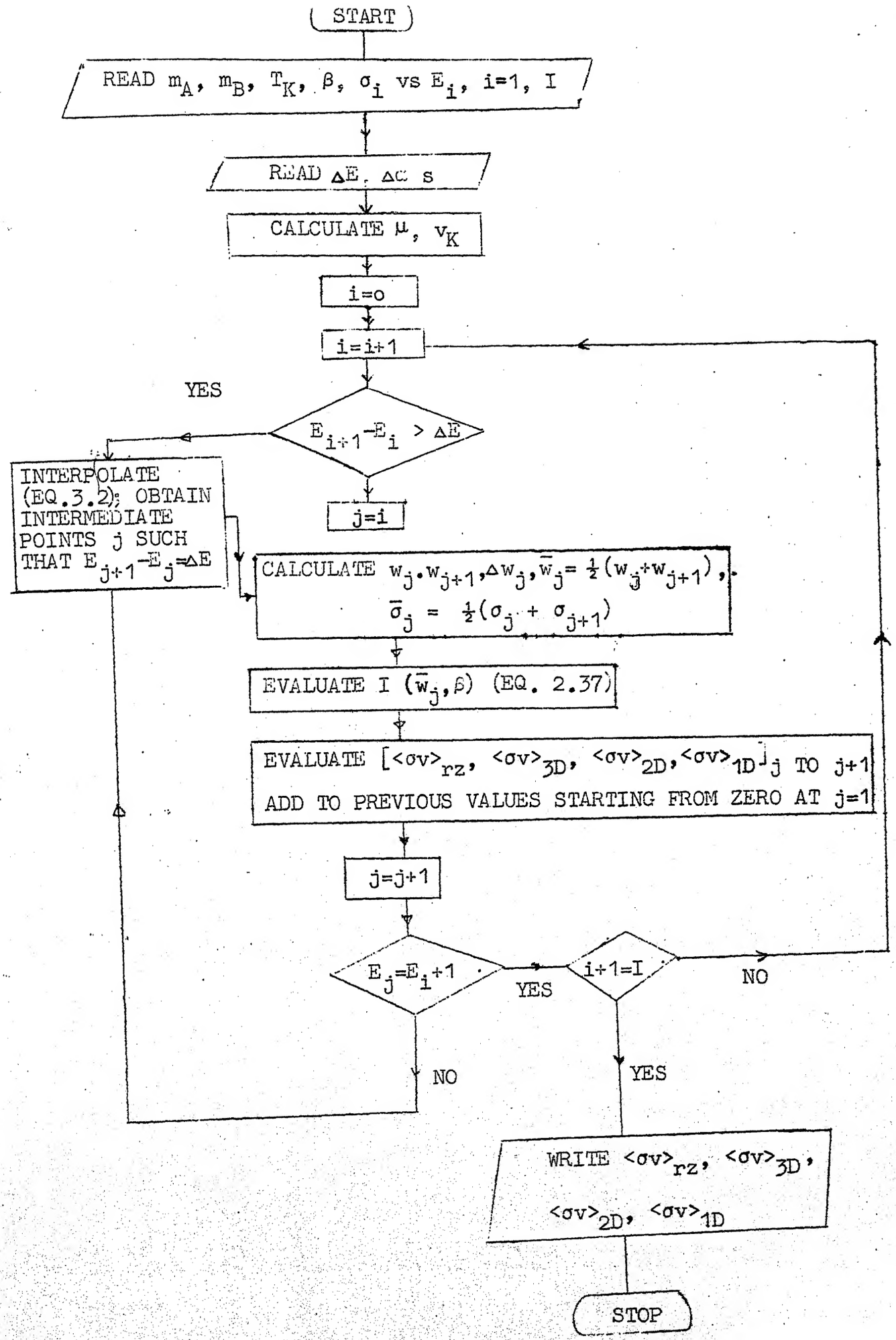

FIG.3.2 : Outline of the computer program used to evaluate $\langle\sigma v\rangle$

small intervals of α were needed to obtain desired accuracy. For most calculations 20 to 50 uniform intervals of α over the range o to 1 were adequate. But for small values of β, as many as 1000 intervals of α were needed. Further, it was found to be the best to merge the exponential in Eq. 2.36 with the exponential in Eq. 2.37 for the purposes of integration, and to use non-uniform intervals of α. Relatively large intervals in the range o to 0.8 and finer intervals in the range 0.8 to 1 gave good and fast results.

The correctness of the calculations was verified by the following considerations :

1. The values of $\langle\sigma v\rangle_{rz}$ given by Eqs. 2.36 and 2.37 for $\beta \longrightarrow o$ and $\beta \longrightarrow \infty$ were calculated and compared with the limiting results of Eqs. 2.39 and 2.40 respectively. Calculations were improved until accurate agreement was achieved upto $\beta = 10^{-3}$ to $\beta = 10^{3}$. Since these were the worst cases, the accuracy of the calculations for other values of β could obviously be assumed.

2. For $\beta = 1$, $\langle\sigma v\rangle_{rz}$ of Eq. 2.36 should correspond to $\langle\sigma v\rangle_{3D}$ of Eq. 2.38. This was checked. These values were further compared with the $\langle\sigma v\rangle$ values given in Ref. [1] for 3-dimensional Maxwellian distribution of velocities. Expected agreement was found, as will be reported later.

3. If we put $\sigma(w) = 1$, then Eqs. 2.36 to 2.40 can be integrated analytically or through the use of tabulated error function for $\beta = 1$, o and ∞. The results thus obtained agreed with the computed results for these cases. Here we may point out that actual limits of integration with respect to w in Eqs. 2.36 and 2.38 to 2.40 are not o to ∞, but correspond to deuteron energy values from 7 to 1000 keV, as the data available was limited to this range (see Appendix B).

3.3 RESULTS AND DISCUSSIONS

$\langle\sigma v\rangle$ - calculations were done for the DT, DD and DHe^3 fusion reactions for the Maxwellian and non-Maxwellian velocity distributions, with a view to see the effect on $\langle\sigma v\rangle$ of a departure of velocity distribution from Maxwellian. The departures considered were limited to those which could be described by a two-temperature pseudo-Maxwellian distribution as discussed in Section 2.5. The values of $\langle\sigma v\rangle$ for different distributions are then compared for the same value of T_K, the kinetic temperature, as discussed in Section 2.7. We summarize the results in the following subsections.

3.3.1 $\langle\sigma v\rangle$ FOR 1-D, 2-D and 3-D MAXWELLIAN Distribution

The values of $\langle\sigma v\rangle$ available in literature are for 3-dimensional Maxwellian distributions. These are listed in the last columns of Tables 3.4 to 3.6, taken from Ref. [1].

Table 3.4

$\langle\sigma v\rangle_{DT}$ for 1-D, 2-D and 3-D Maxwellian velocity distribution

S.No.	T_K keV	$\langle\sigma v\rangle_{1D} \times 10^{22}$ $m^3 s^{-1}$	$\langle\sigma v\rangle_{2D} \times 10^{22}$ $m^3 s^{-1}$	$\langle\sigma v\rangle_{3D} \times 10^{22}$ $m^3 s^{-1}$	$\langle\sigma v\rangle_{3D} \times 10^{22}$ REF [1] $m^3 s^{-1}$
1.	5	0.477	0.226	0.135	0.14
2.	10	1.78	1.40	1.12	1.1
3.	20	3.95	4.34	4.38	4.3
4.	30	5.22	6.48	7.09	6.5
5.	50	6.40	8.64	9.95	8.4
6.	100	6.88	9.43	10.8	8.1

Table 3.5

$\langle\sigma v\rangle_{DD}$ for 1-D, 2-D and 3-D Maxwellian velocity distribution

S.No.	T_K keV	$\langle\sigma v\rangle_{1D} \times 10^{23}$ $m^3 s^{-1}$	$\langle\sigma v\rangle_{2D} \times 10^{23}$ $m^3 s^{-1}$	$\langle\sigma v\rangle_{3D} \times 10^{23}$ $m^3 s^{-1}$	$\langle\sigma v\rangle_{3D} \times 10^{23}$ REF [1] $m^3 s^{-1}$
1.	5	0.049	0.025	0.017	0.015
2.	10	0.205	0.142	0.114	0.086
3.	20	0.637	0.535	0.484	0.36
4.	30	1.11	1.01	0.953	0.64
5.	50	1.94	2.01	1.98	1.35
6.	100	3.00	3.90	4.28	3.0

Table 3.6

$\langle\sigma v\rangle_{DHe^3}$ for 1-D, 2-D and 3-D Maxwellian velocity distribution

S.No.	T_K keV	$\langle\sigma v\rangle_{1D} \times 10^{23}$ $m^3\ s^{-1}$	$\langle\sigma v\rangle_{2D} \times 10^{23}$ $m^3\ s^{-1}$	$\langle\sigma v\rangle_{3D} \times 10^{23}$ $m^3\ s^{-1}$	$\langle\sigma v\rangle_{3D} \times 10^{23}$ REF [1] $m^3\ s^{-1}$
1.	5	0.014	0.002	6×10^{-4}	10^{-6}
2.	10	0.184	0.051	0.023	0.024
3.	20	1.34	0.624	0.374	0.32
4.	30	3.13	2.00	1.41	1.1
5.	50	6.64	6.11	5.32	4.4
6.	100	11.4	14.8	16.3	17.0

In the columns just preceding the last columns, are listed the results of our calculations [Eq. 2.38]. It is seen that there is general agreement. However, in view of the fact that the input data (Appendix B) used for all our calculations is also from Ref. [1], better agreement could be expected. We do not wish to stress this comparison too much, except to note that if the input data is as in Appendix B, then $\langle\sigma v\rangle_{3D}$ values should be as calculated here.

Our main interest here is to see the effect of departure from Maxwellian distribution on $\langle\sigma v\rangle$. For this purpose we list in the same Tables 3.4 to 3.6, the calculated values of $\langle\sigma v\rangle_{1D}$ and $\langle\sigma v\rangle_{2D}$, as calculated in accordance with Eqs. 2.39 and 2.40. As already noted in Chapter 2, these are extreme forms of the two-temperature pseudo-Maxwellian distribution as $\beta \longrightarrow 0$ or ∞ respectively. This is hardly a situation which would ever exist in practice, but establishes the upper bounds of the effect on $\langle\sigma v\rangle$ of possible departures from Maxwellian distribution.

As we see from Tables 3.4 to 3.6, $\langle\sigma v\rangle_{1D}$ and $\langle\sigma v\rangle_{2D}$ can be significantly larger than $\langle\sigma v\rangle_{3D}$ upto a certain temperature T_K. This temperature is about 10 keV for DT reaction and about 30 keV for DD and DHe^3 reactions. In view of the fact that these are the temperatures of practical interest in thermonuclear fusion, we arrive at the conclusion that 1-D and 2-D Maxwellian distribution of velocities give enhanced reaction

rates for all the three fusion reactions. However, at lighter temperatures, the reverse effect is seen.

These effects can be explained as follows. For the same kinetic temperature T_K, the average relative speed is highest in 1-D and lowest in 3-D Maxwellian distributions. At lower values of T_K, this contributes positively to $\langle \sigma v \rangle$ as σ increases with v. But beyond a certain v, σ decreases with v. This is apparent from Appendix B only for DT reaction. However, the same thing happens for DD and DHe^3 reactions if we push the data beyond 1000 keV in Appendix B. In any case, as far as numerical calculations in this work are concerned, σ is taken to be zero beyond 1000 keV.

Thus at higher T_K, the gain in v actually reduces $\langle \sigma v \rangle$.

3.3.2 $\langle \sigma v \rangle$ For a Two-Temperature Pseudo-Maxwellian Distribution

Figs. 3.3 to 3.7 plot $\langle \sigma v \rangle_{rz}$ of Eq. 2.36 as a function of the parameter $\beta = T_r/T_z$. As can be seen from the figures, while β is varied, the kinetic temperature, $T_K = \frac{2}{3} \left(\frac{1}{2} T_z + T_r \right)$ is kept fixed. The meaning of this is, that as the radial and axial temperatures are varied, the average kinetic energy per particle is kept fixed, T_K being a measure for the same. This has already been discussed in Section 2.7.

Figs. 3.3 plots the results for the DT reaction at 5 keV and for the DD reaction at 30 keV, the temperatures of maximum

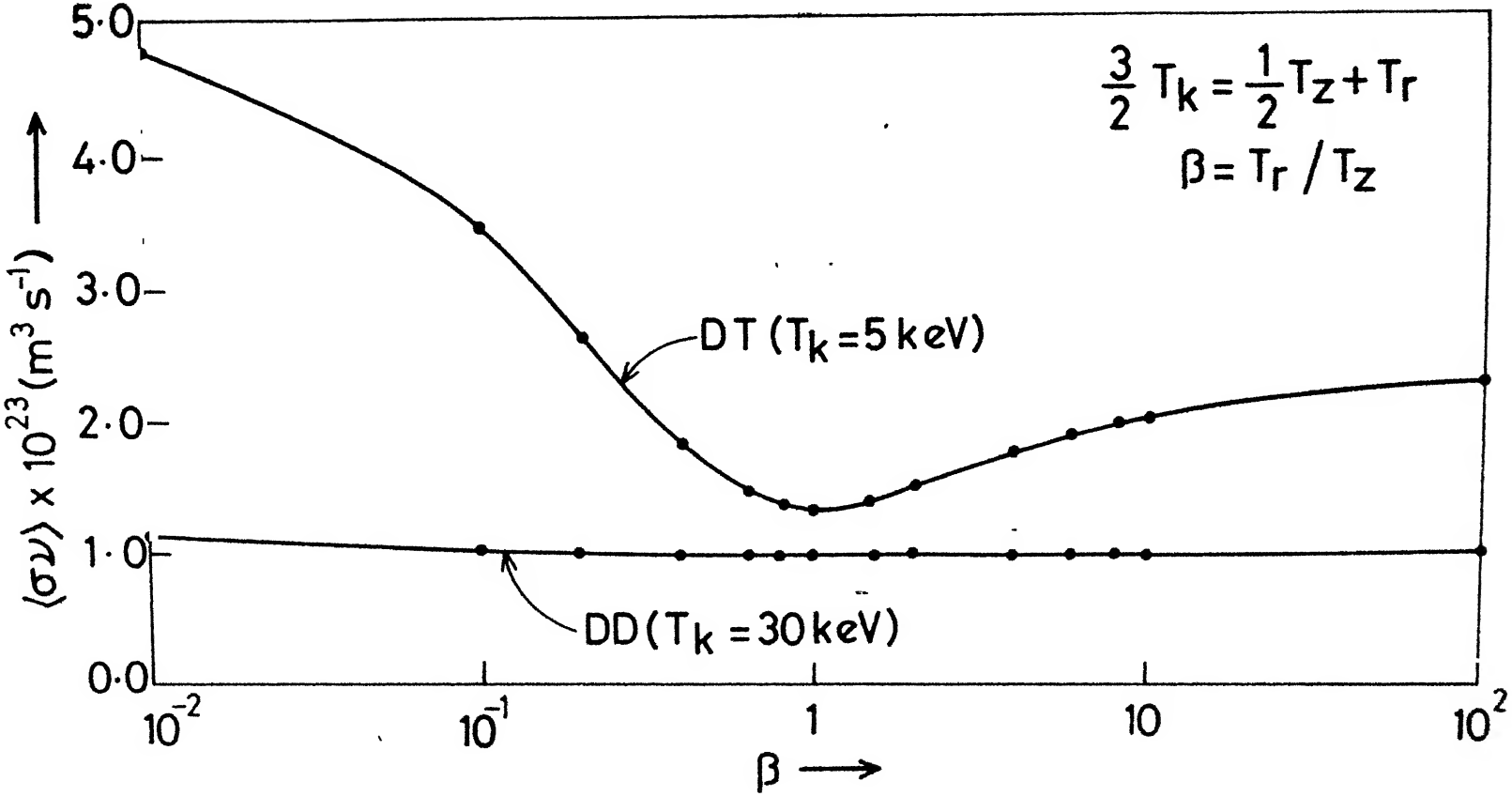

FIG: 3·3 Variation of $\langle\sigma v\rangle$ with β for DT and DD reactions at temperatures $T_k = 5$ and $T_k = 30$ keV

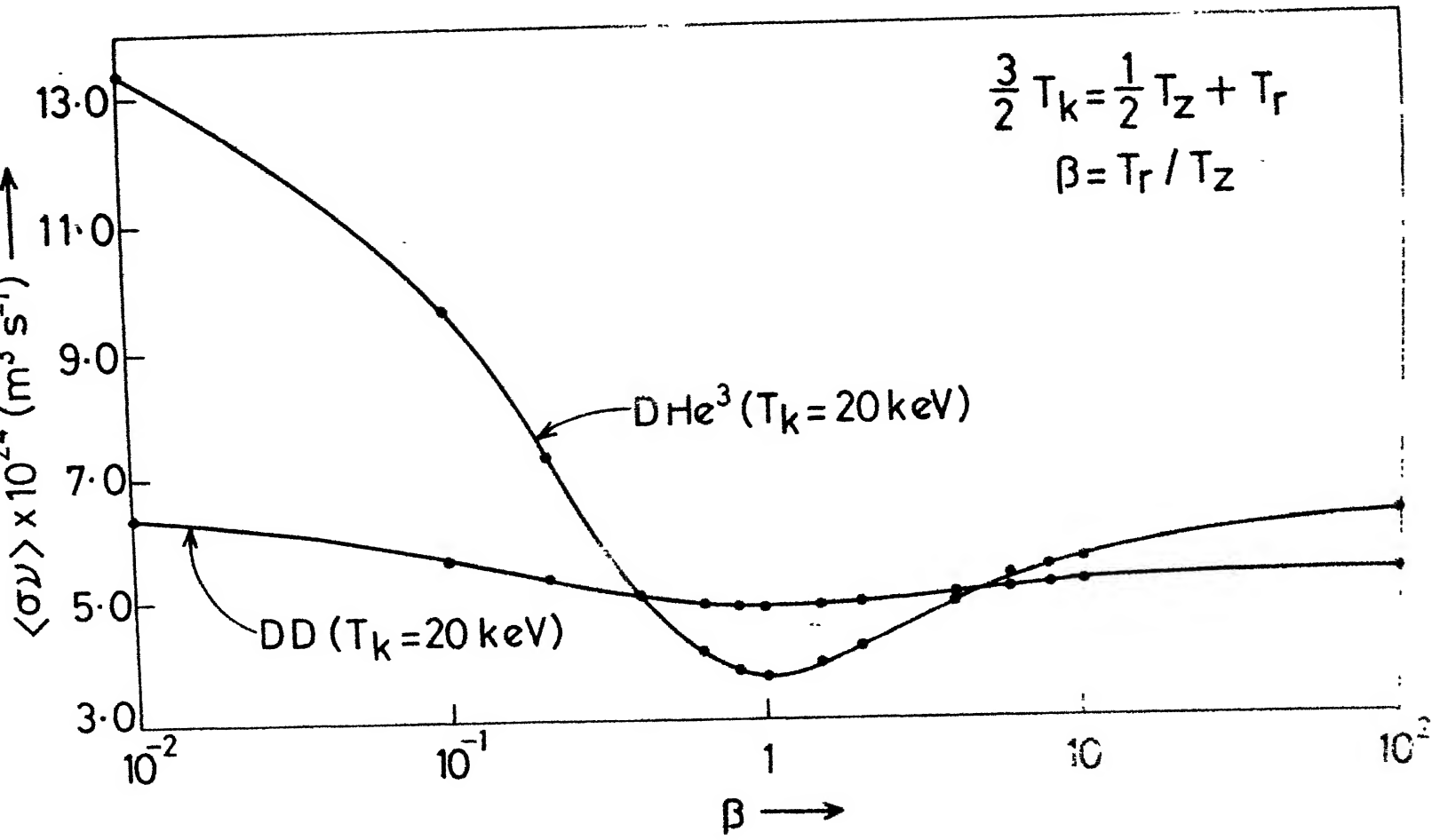

FIG. 3·4 Variation of $\langle \sigma v \rangle$ with β for DD and DHe^3 reactions at temperatures $T_k = 20$ and $T_k = 20$ keV.

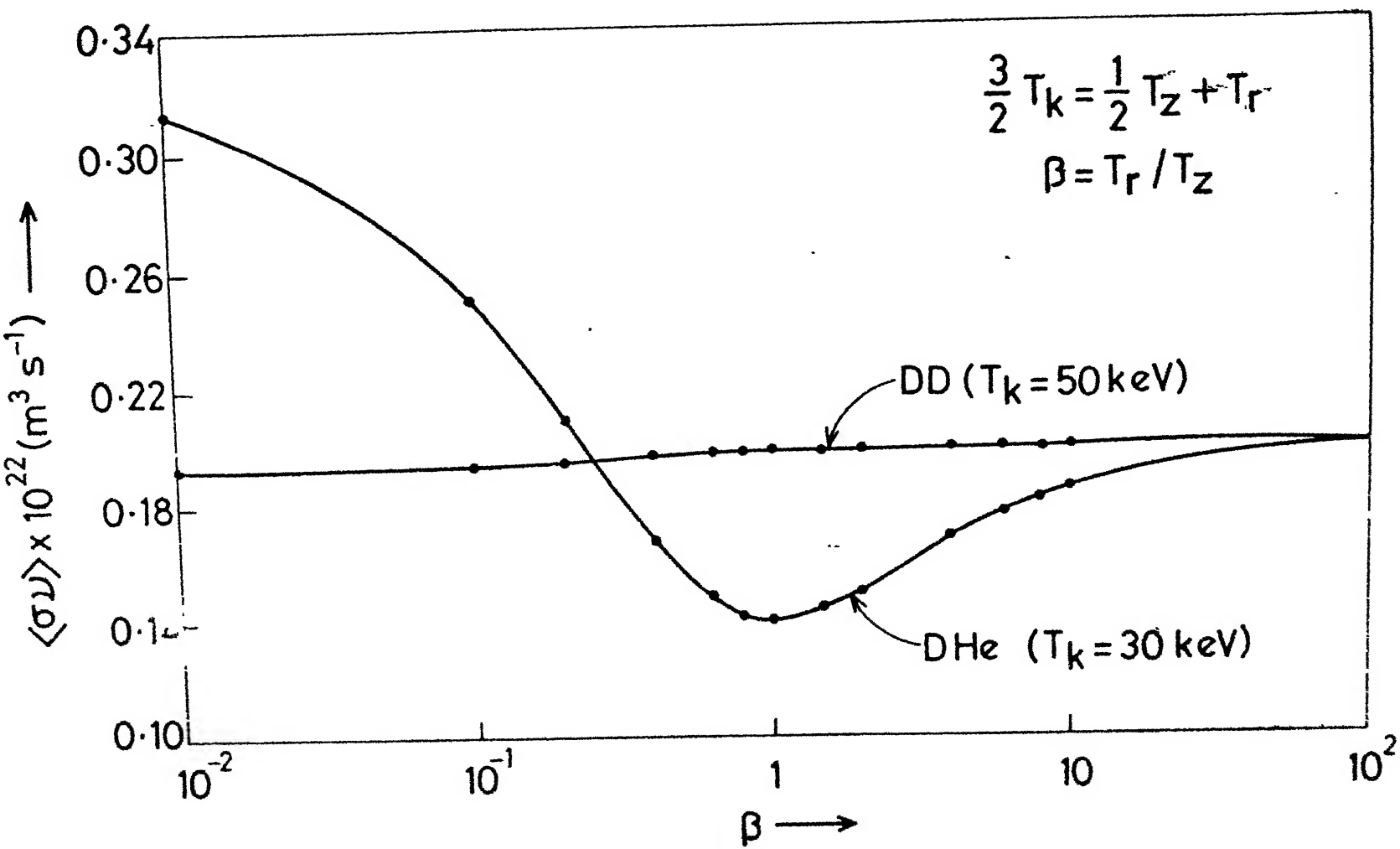

FIG. 3·5 Variation of $\langle\sigma v\rangle$ with β for DD and DHe^3 reactions at temperatures T_k = 50 and T_k = 30 keV.

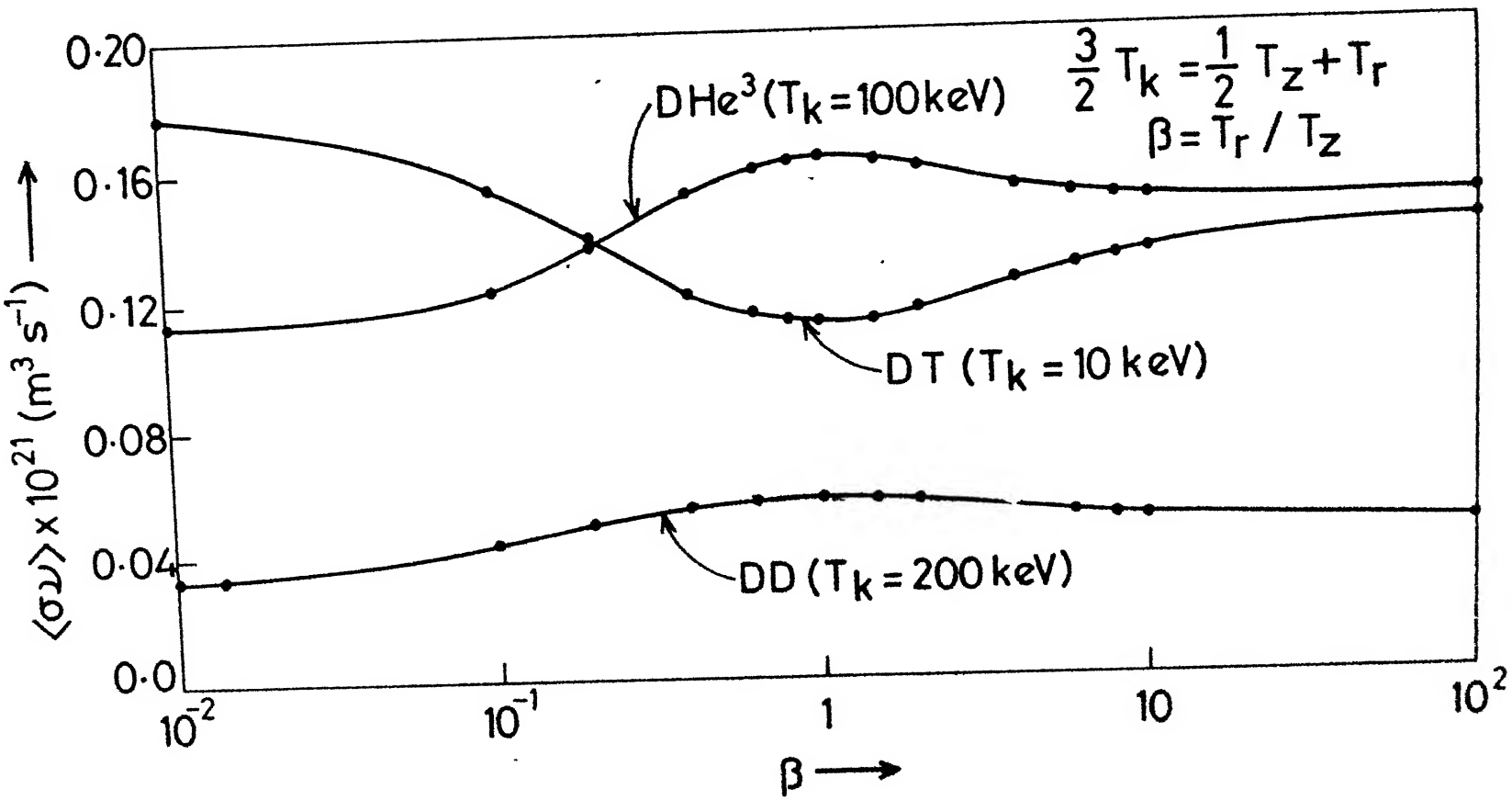

FIG. 3·6 Variation of $\langle\sigma v\rangle$ with β for DT, DD and DHe^3 reactions at temperatures T_k = 10, T_k = 200 and T_k = 100 keV.

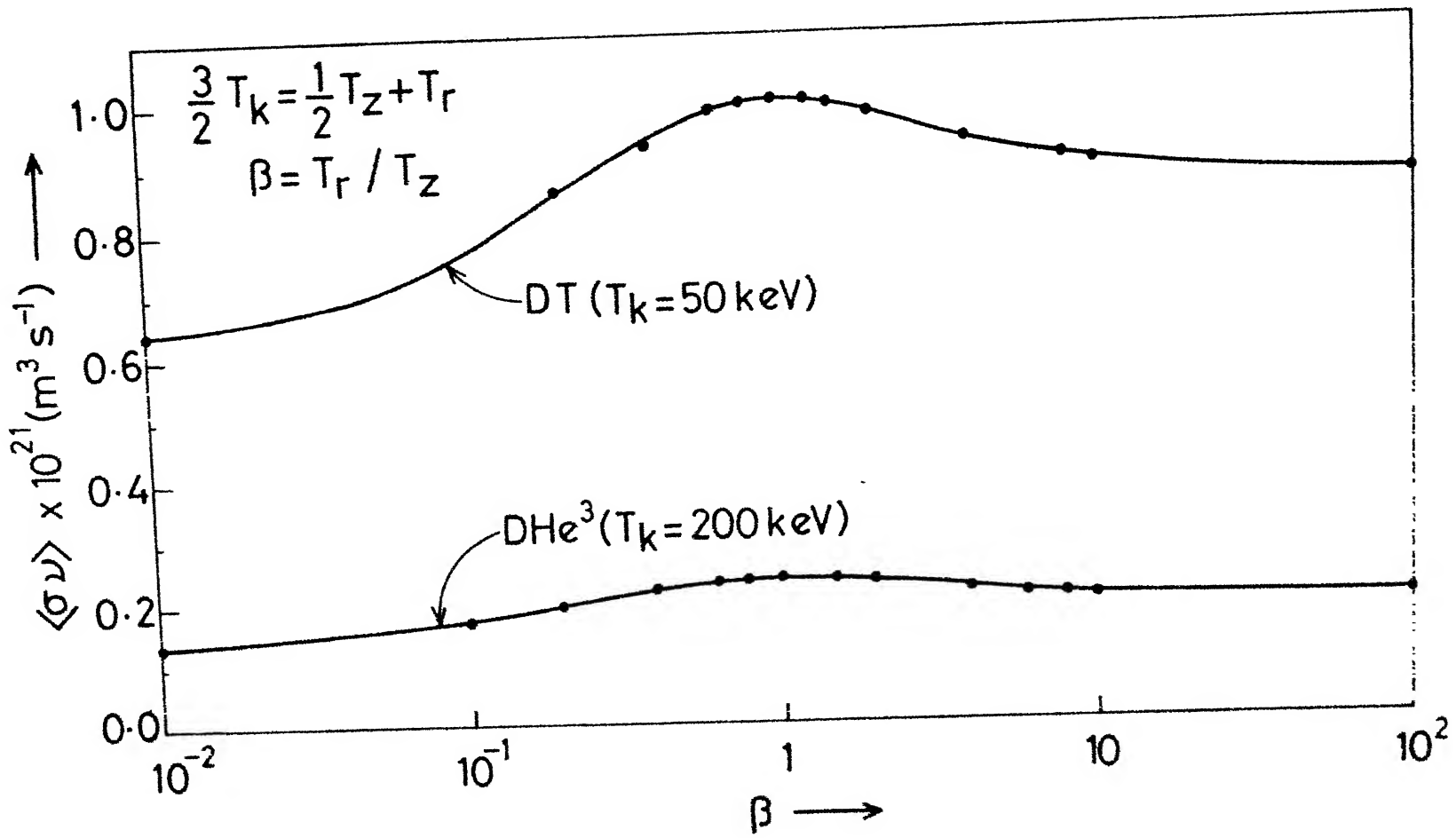

FIG: 3·7 Variation of $\langle\sigma\nu\rangle$ with β for DT and DHe^3 reactions at temperatures T_k= 50 and T_k= 200 keV.

interest in nuclear fusion for these reactions, respectively. In the vicinity of the 3-D Maxwellian distribution, enhancement in the $\langle \sigma v \rangle$ for DT reaction at 5 keV is seen to be more than 20% ($\beta \sim 0.5$ to 2.0). The enhancement for the DD reaction at 30 keV is, however, only about 1%. It is seen that the reaction rate is enhanced if $T_r \neq T_z$, no matter which is more. This can also be confirmed by differentiating $\langle \sigma v \rangle_{rz}$ in Eq. 2.36 partially w.r.t. β. It shows an extremum at $\beta=1$, as is also apparent from the computer results shown in Figs. 3.3 to 3.7.

Figs. 3.4 and 3.5 show similar data for DD and DHe^3 reactions, at some chosen values of T_K. Again an enhancement in $\langle \sigma v \rangle$ value due to deviation from Maxwellian distribution is seen.

Fig. 3.6 gives the results for DT reaction at 10 keV, another temperature of practical interest for nuclear fusion. An enhancement of the order of 10% in the vicinity of $\beta=1$ is noted. In this figure, we also give the results for DHe^3 reaction at 100 keV and DD reaction at 200 keV. These temperatures can be of practical interest in the next generation fusion reactors when attainment of such high temperatures becomes feasible. It is to be noted, however, that for these cases, deviation from 3-D Maxwellian leads to a reduction in $\langle \sigma v \rangle$. The same is the case with the results shown in Fig. 3.7. This has already been explained qualitatively in Section 3.3.1 in connection with the Tables 3.4 to 3.6.

Figs. 3.8 to 3.11 show $\langle\sigma v\rangle$ vs T_K with β as a parameter. Since $\langle\sigma v\rangle$ changes fast with T_K, a narrow range of temperature is chosen for each plot, so the difference in $\langle\sigma v\rangle$ for different values of β can be displayed with clarity. The temperatures chosen are the ones of most practical interest, e.g. 10 keV for the DT reaction in Fig. 3.8 and $\sim$ 30 keV for the DD and DHe^3 reactions in Figs. 3.9 and 3.10. It can be seen that for $\beta=1$, the $\langle\sigma v\rangle$ is lowest, and it is larger for both β = 0.5 and 2.0. $\beta \longrightarrow$ o yields the highest value of $\langle\sigma v\rangle$ followed by the value corresponding to $\beta \longrightarrow \infty$. Finally, in Fig. 3.11, a representative plot of $\langle\sigma v\rangle$ vs T_K is given where the reverse is true.

A summary of the important conclusions of this chapter together with some suggestions is presented briefly in the next chapter.

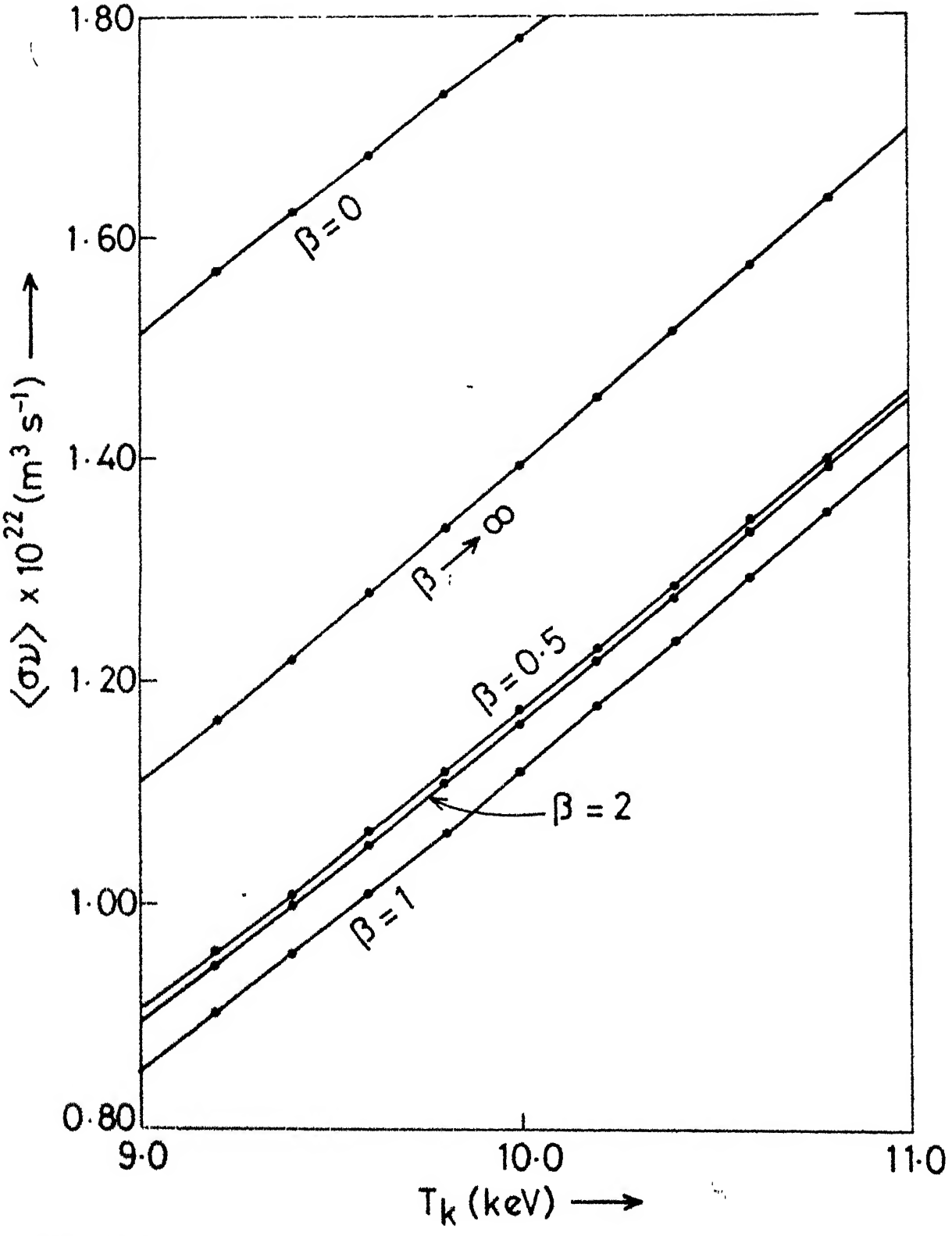

FIG. 3·8 Variation of $\langle\sigma v\rangle_{DT}$ Vs T_k with β as a parameter.

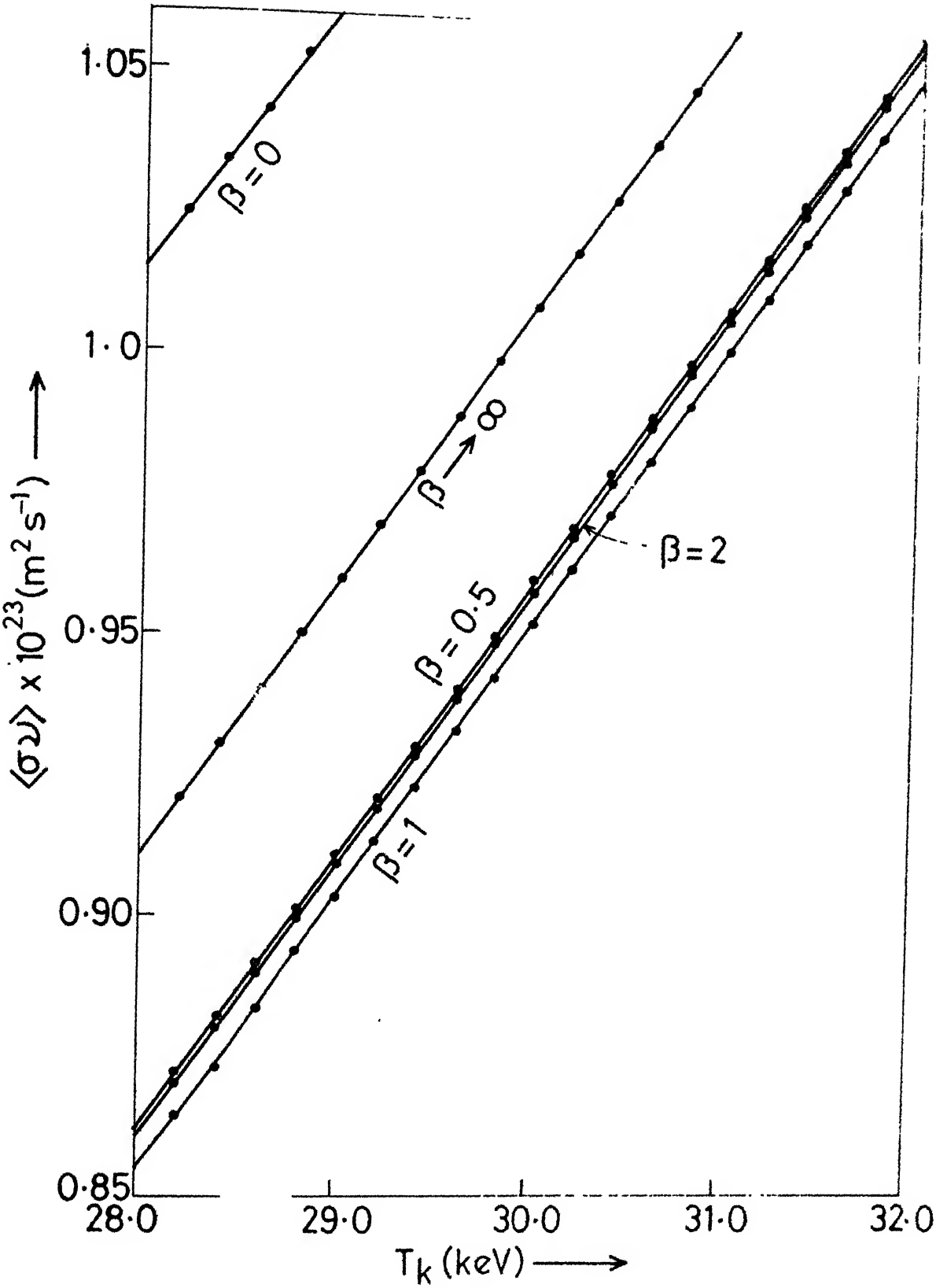

FIG. 3·9 Variation of $\langle\sigma v\rangle_{DD}$ Vs. T_k with β as a parameter.

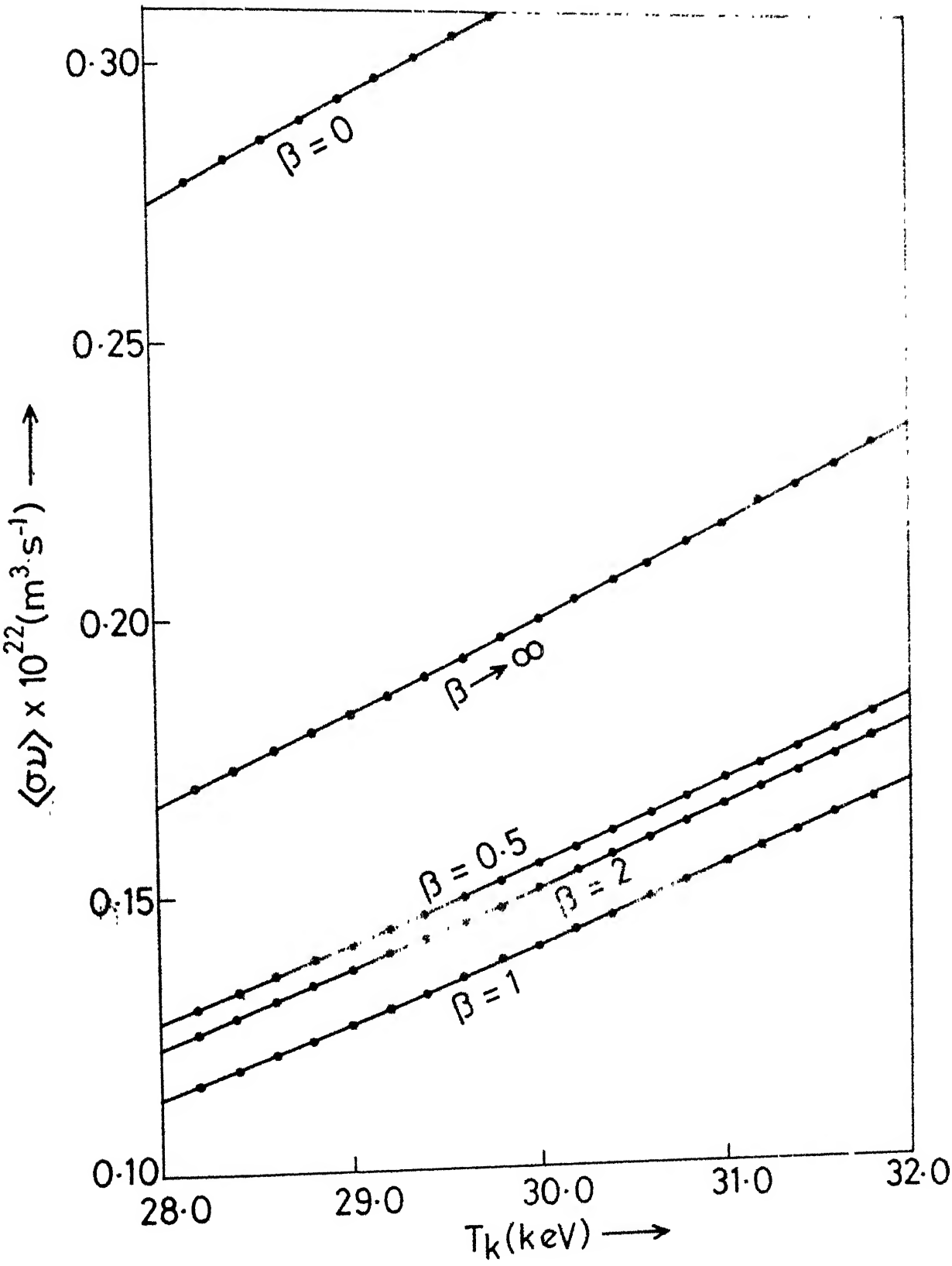

FIG: 3·10 Variation of $\langle\sigma\nu\rangle_{DHe^3}$ Vs T_k with β as a parameter.

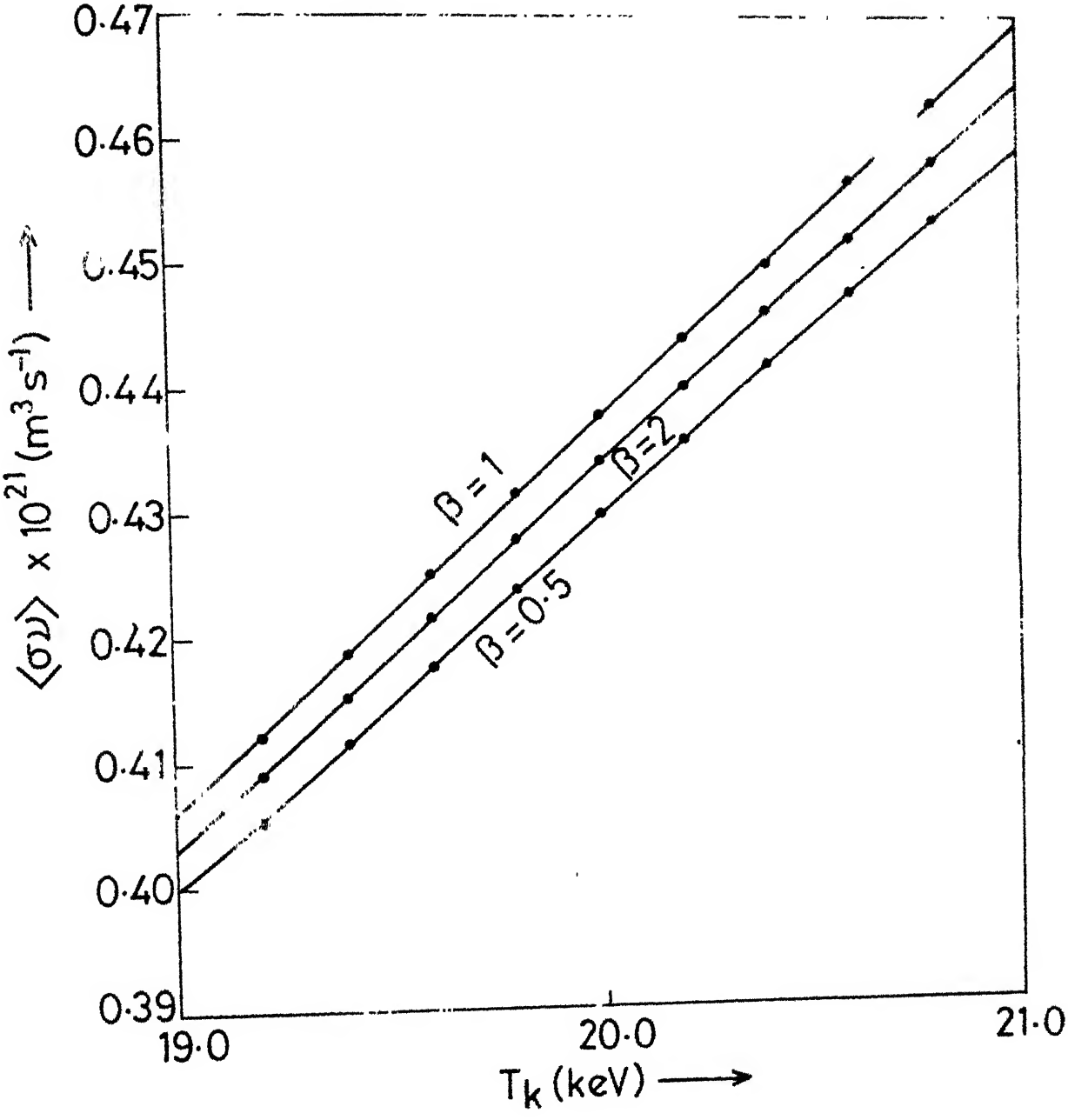

FIG. 3·11 Variation of $\langle\sigma v\rangle_{DT}$ Vs T_k with β as a parameter.

Chapter 4

SUMMARY AND SUGGESTIONS

4.1 SUMMARY

After a brief introduction to the present work in Chapter 1, we presented a detailed analysis of the problem of calculating fusion reaction rates under non-Maxwellian conditions in Chapter 2.

In Sections 2.1 and 2.2, the basic equations were written down and the underlying assumptions and their validity was discussed. The basic equations were then used in Section 2.3 to calculate $\langle \sigma v \rangle$ for 1-, 2- and 3-dimensional Maxwellian distributions. The expressions for these cases are relatively easy to establish. To develop a suitable expression for $\langle \sigma v \rangle$ for a general two-temperature pseudo-Maxwellian velocity distribution (Section 2.5), transformation to CM and relative velocity coordinates was done (Section 2.4). The final expression was then obtained in Section 2.6. We further discussed the basis of comparison for different values of $\langle \sigma v \rangle$ in Section 2.7. In Section 2.8, suitable dimensionless parameters were introduced in the various expressions developed.

In Chapter 3, various details of the numerical computations were discussed. The results were presented and discussed in Section 3.3. The main conclusions are given below.

4.2 CONCLUSIONS

The calculations reported in this work indicate that the fusion reaction rates for the DT, DD and DHe^3 reactions are enhanced if the velocity distribution deviates from the thermodynamic Maxwellian distribution, at temperatures of maximum practical interest. For example for the DT reaction, the reaction rate may be enhanced by 10 to 20% in the temperature range of 5 to 10 keV. Similar conclusion is valid for the DHe^3 reaction for 20 to 40 keV range. Enhancement in the DD reaction rate is however seen to be rather small (see Section 3.3 for details).

We should stress, however, that the above conclusions are based on considering deviations in the form of a two-temperature pseudo-Maxwellian distribution. Their validity for arbitrary deviations will need to be verified by additional computations and/or analytical techniques.

The calculations reported here also show that at higher temperatures (more than 20 keV for DT and more than 40 keV for DD and DHe^3 reactions), the deviation from Maxwellian distribution reduces the reaction rates, in contrast to the opposite effect at lower temperature mentioned above.

4.3 SUGGESTIONS

1. In this work we have considered only two-temperature pseudo-Maxwellian distributions. Arbitrary departures from

Maxwellian distribution need to be considered to draw stronger conclusions.

2. Under certain conditions (see Ref.[11]), a strong non-Maxwellian tail is superimposed on the Maxwellian distribution. The effect of this on the fusion reaction rates can be investigated very much along the lines of this work.

3. The validity of the present calculations breaks down at the very high densities encountered in inertial fusion due to correlation effects. This should be incorporated in the conclusions. [see Section 2.2]

4. As was mentioned in Section 2.2, the polarization effects are known to enhance fusion reaction rates by as much as a factor of two under suitable conditions. This should also be investigated.

5. For all the calculations we have used the data shown in Appendix B. There appears to be some need to improve this data in view of the discussions in Section 3.1. Furthermore, we have used a sharp cut-off at 7 and 1000 keV. This range could be enlarged by extending the least squares approximation curve. This will have some effect on $\langle \sigma v \rangle$ at very low temperatures (1 to 5 keV) or at very high temperatures (above, say, 100 or 200 keV).

APPENDIX A

A1 Proof of $d^3v_1\, d^3v_2 = d^3V\, d^3v$ [i.e. from Eq. 2.4b]

From Eqs. 2.16 and 2.17, we have,

$$v_x = v_{x_2} - v_{x_1}$$

$$v_y = v_{y_2} - v_{y_1}$$

$$v_z = v_{z_2} - v_{z_1}$$

$$V_x = \mu_A v_{x_1} + \mu_B v_{x_2}$$

$$V_y = \mu_A v_{y_1} + \mu_B v_{y_2}$$

$$V_z = \mu_A v_{z_1} + \mu_B v_{z_2} \qquad \text{(a1.1)}$$

where

$$\mu_A = \frac{m_A}{m_A + m_B}$$

and

$$\mu_B = \frac{m_B}{m_A + m_B}$$

By using the definition of Jacobian $\left| \frac{\partial (\vec{v}, \vec{V})}{\partial (\vec{v}_1, \vec{v}_2)} \right|$, we can write,

$$J = \frac{\partial (\vec{v}, \vec{V})}{\partial (\vec{v}_1, \vec{v}_2)}$$

or

$$J = \begin{bmatrix} \frac{\partial v_x}{\partial v_{x_1}} & \frac{\partial v_y}{\partial v_{x_1}} & \frac{\partial v_z}{\partial v_{x_1}} & \frac{\partial V_x}{\partial v_{x_1}} & \frac{\partial V_y}{\partial v_{y_1}} & \frac{\partial V_z}{\partial v_{x_1}} \\ \frac{\partial v_x}{\partial v_{y_1}} & \frac{\partial v_y}{\partial v_{y_1}} & \frac{\partial v_z}{\partial v_{y_1}} & \frac{\partial V_x}{\partial v_{y_1}} & \frac{\partial V_y}{\partial v_{y_1}} & \frac{\partial V_z}{\partial v_{y_1}} \\ \frac{\partial v_x}{\partial v_{z_1}} & \frac{\partial v_y}{\partial v_{z_1}} & \frac{\partial v_z}{\partial v_{z_1}} & \frac{\partial V_x}{\partial v_{z_1}} & \frac{\partial V_y}{\partial v_{z_1}} & \frac{\partial V_z}{\partial v_{z_1}} \\ \frac{\partial v_x}{\partial v_{x_2}} & \frac{\partial v_y}{\partial v_{x_2}} & \frac{\partial v_z}{\partial v_{x_2}} & \frac{\partial V_x}{\partial v_{x_2}} & \frac{\partial V_y}{\partial v_{x_2}} & \frac{\partial V_z}{\partial v_{x_2}} \\ \frac{\partial v_x}{\partial v_{y_2}} & \frac{\partial v_y}{\partial v_{y_2}} & \frac{\partial v_z}{\partial v_{y_2}} & \frac{\partial V_x}{\partial v_{y_2}} & \frac{\partial V_y}{\partial v_{y_2}} & \frac{\partial V_z}{\partial v_{y_2}} \\ \frac{\partial v_x}{\partial v_{z_2}} & \frac{\partial v_y}{\partial v_{z_2}} & \frac{\partial v_z}{\partial v_{z_2}} & \frac{\partial V_x}{\partial v_{z_2}} & \frac{\partial V_y}{\partial v_{z_2}} & \frac{\partial V_z}{\partial v_{z_2}} \end{bmatrix} \quad \text{(a1.2)}$$

The partial derivatives in Eq. a1.2 can be substituted from Eq. a1.1 to obtain

$$\therefore \quad d^3v_1\, d^3v_2 = -\, d^3V\, d^3v$$

A2 Proof of $m_A v_{1i}^2 + m_B v_{2i}^2 = MV_i^2 + \mu v_i^2$ [i.e. Eq. 2.23]

where $i = x, y, \text{ or } z$

$$m_A v_{1i}^2 + m_B v_{2i}^2 = MV_i^2 + \mu\, v_i^2 \qquad (a2.1)$$

Steps

From Eqs. 2.16 and 2.17, we have

$$M\, V_i = m_A\, v_{1i} + m_B\, v_{2i}$$

and

$$v_i = v_{2i} - v_{1i}$$

From where we can have v_{1i} and v_{2i} as

$$v_{1i} = \frac{MV_i - m_B\, v_i}{M}$$

and

$$v_{2i} = \frac{MV_i + m_B\, v_i}{M}$$

Hence, the left hand side of the above Eq. a2.1 can be written as,

$$m_A v_{1i}^2 + m_B v_{2i}^2 = m_A \left[\frac{MV_i - m_B v_i}{M}\right]^2 + m_B \left[\frac{MV_i + m_A v_i}{M}\right]^2$$

$$= \frac{1}{M^2} \left[m_A (MV_i - m_B v_i)^2 + m_B (MV_i + m_A v_i)^2 \right]$$

$$= \frac{1}{M^2} \left[m_A M^2 V_i^2 + m_A m_B^2 v_i^2 + m_B M^2 V_i^2 + m_A^2 m_B v_i^2 \right]$$

$$= \frac{1}{M^2} \left[M^2 V_i^2 (m_A + m_B) + m_A m_B v_i (m_A + m_B) \right]$$

$$= M V_i^2 + \frac{m_A m_B}{M} v_i$$

$$= M V_i^2 + \mu v_i$$

$$= \text{R.H.S.}$$

Thus,

$$m_A v_{1i}^2 + m_B v_{2i}^2 = M V_i^2 + \mu v_i^2$$

APPENDIX B

TABULATED VALUES OF σ_{DT}, σ_{DD} and σ_{DHe^3} USED FOR CALCULATIONS REPORTED IN THIS WORK (FROM REF.[1])

S.No.	Deuteron Energy, E_D keV	$\sigma_{DT} \times 10^{28}$ m^2	$\sigma_{DD} \times 10^{28}$ m^2	$\sigma_{DHe^3} \times 10^{28}$ m^2
1.	7.00	0.00010	0.0	0.0
2.	8.00	0.00044	0.0	0.0
3.	9.00	0.00099	0.0	0.0
4.	10.00	0.0018	0.0	0.0
5.	20.00	0.055	0.00054	0.0
6.	30.00	0.280	0.00222	0.0
7.	40.00	0.710	0.005	0.000245
8.	50.00	1.40	0.00849	0.000924
9.	60.00	2.20	0.013	0.00225
10.	70.00	3.05	0.0175	0.00473
11.	80.00	3.85	0.0222	0.0082
12.	90.00	4.45	0.0270	0.0135
13.	100.00	4.80	0.0315	0.0197
14.	200.00	4.00	0.0640	0.185
15.	300.00	2.30	0.0848	0.480
16.	400.00	1.40	0.108	0.724
17.	500.00	1.05	0.120	0.780
18.	600.00	0.750	0.135	0.648
19.	700.00	0.580	0.141	0.490
20.	800.00	0.450	0.152	0.369
21.	900.00	0.350	0.170	0.300
22.	1000.00	0.310	0.180	0.244

APPENDIX C

TABLE OF SOME CONSTANTS AND CONVERSION FACTORS USED IN THIS WORK

$m_D = 2.0141$ u

$m_T = 3.01605$ u

$m_{He^3} = 3.01603$ u

1 u = 1.660438×10^{-27} Kg.

1 keV = 1.602×10^{-16} u

h = 6.626×10^{-34} J-s

$N_o = 6.022 \times 10^{26}$ K-mol^{-1}

e = 1.602×10^{-19} C

$\varepsilon_o = 8.854 \times 10^{-12}$ $C^2N^{-1}m^{-2}$

C = 2.998×10^{8} ms^{-1}

1 barn = 10^{-28} m^2

REFERENCES

[1] S. Glasstone and R.H. Lovberg (1960) Controlled Thermonuclear Reactions : An introduction to theory and experiment.

[2] F.F. Chen (1984) Introduction to Plasma Physics and Controlled Fusion, Vol. I.

[3] R.A. Cairns (1985) Plasma Physics.

[4] N.A. Krall and A.W. Trivelpiece (1973) Principles of Plasma Physics.

[5] T. Kammash (1975) Fusion Reactor Physics : Principles and Technology.

[6] L.D. Landau and E.M. Lifshitz (1980) Statistical Physics : Course of Theoretical Physics, Vol. V.

[7] C.F. Wandel, T. Hesselberg Jensen and O. Kofoed Hansen, Nuclear Instruments and methods 4 (1959), 249-260.

[8] J.N. Anno (1976) Wave Mechanics for Engineers.

[9] Erwin Kreyszig (1972) Advanced Engineering Mathematics.

[10] F.B. Hildrbrand (1976) Advanced Calculus for Applications.

[11] D.A.E. Seminar on Physics of Fusion Plasmas, Matheran (1982).

[12] K. Huang (1963), Statistical Mechanics.

[13] F.B. Hildebrand (1974) Introduction to Numerical Analysis.

NETP-1986-M-AGA-NYC